

Supplementary Information

A laboratory study on the uptake of gaseous molecular iodine by clay minerals at different relative humidities

Shuzo Kutsuna* and Naoki Kaneyasu

National Institute of Advanced Industrial Science and Technology (AIST),

16–1 Onogawa, Tsukuba, Ibaraki 305 8569, JAPAN

1. SUPPORTING INFORMATION FOR SECTION 2.2

S1.1. Experimental Conditions

Table S1. Experimental flow rates and mass-flow controllers

Flow (Fig. 1)	Mass-flow controller	gas	Flow rate at 298.2 K ($10^{-3} \text{ dm}^3 \text{ s}^{-1}$)			
			20% RH	50% RH	80% RH	96% RH
F4	SEC-E40 ^a	air	5.5341	3.3496	1.1651	0
F5	SEC-E40 ^a	humidified air	1.4706 ^c	3.6214 ^c	5.8274 ^c	7.0590 ^c
F1	SEC-400MK3 ^a	air			0.1790	
F2	SEC-400MK3 ^a	air			0.2078	
F3	SEC-E40 ^a	CO ₂ -air			0.2856	
F6	type 11598 ^b	air			0.0242	
F7	SEC-400MK3 ^a	air			1.6534	
F8	SEC-400MK3 ^a	air			1.6591	
$F_{\text{out}} = F3 + F4 + F5 + F6$			7.3145	7.2808	7.3023	7.3688

^a Purchased from HORIBA STEC.; ^b Purchased from MKS.

^c Each value is (F5 of air) + (flow rate of water vapor, 1.2% by volume).

S1.2. Calibration of I₂-Air Mixtures and IBBCEAS System. The partial pressure of I₂ in I₂-air(o), $P_{\text{in-o}}$, was determined by bubbling I₂-air(o) into 20 mL of 20 mM aqueous NaOH solution in an impinger (Figure 1, *f*). I₂ was transformed into I⁻ and IO₃⁻ according to reaction R2. The I⁻ and IO₃⁻ concentration produced in the solutions was determined with an ion chromatograph (Dionex ICS-2100, Thermo Fisher Scientific) in which an aqueous KOH solution was used at a flow rate of 1.0 mL min⁻¹ to elute I⁻ and IO₃⁻ from the IonPac AS-20 column (4 mm i.d., 250 mm long) at 308 K. The KOH concentration was gradually increased from 2.5 to 45 mM according to a timed program. Four experimental runs were conducted (Table S2). A second impinger installed downstream from the first one was used to verify the high efficiency of the bubbling system in trapping gaseous I₂. Concentrations of I⁻ and IO₃⁻ in the second impinger were below detection limits. Molar ratios of I⁻ to IO₃⁻ were within 3% of the ratio expected from reaction R2.

The value of $P_{\text{in-o}}$ was calculated at 7.08 ± 0.09 Pa from the IO₃⁻ concentration, and the volume of I₂-air(o) introduced into the solution as the average of four measurements. Errors represent a standard deviation. Uncertainty of $P_{\text{in-o}}$ was estimated at about 3% (± 0.21 Pa) because molar ratios of I⁻ to IO₃⁻ were within 3% of the ratio expected from reaction R2. From this value, the partial pressure of I₂ in the synthetic air passing through the PFA bottle (Figure 1, *a*) was calculated at 15.3 ± 0.05 Pa, or 0.88 times the saturated vapor pressure (17.14 Pa) of I₂ reported at the preset temperature (288.2 K),¹ and the partial pressure of I₂ in I₂-air(s), with P_0 as P_{in} with a syringe pump speed (F_s) of 4.17×10^{-5} dm³ s⁻¹, was calculated at 40.5 ± 1.2 mPa, for a 0.40 ± 0.01 ppmv concentration.

Table S2. Concentrations of I⁻ and IO₃⁻ in aqueous NaOH into which I₂-air(o) was bubbled.

Run No	Procedure for introducing I ₂ -air(o)			I ⁻ (ppmw) ^a	IO ₃ ⁻ (ppmw) ^a	Mole ratio of I ⁻ /IO ₃ ⁻	Partial pressure of I ₂ in I ₂ -air(o) (Pa) ^b
	Start	Stop	Volume (dm ³)				
1	12:30	13:30	1.3926	43.9	11.8	5.14	7.19
2	13:46	14:50	1.4854	46.0	12.4	5.12	7.08
3	15:05	16:05	1.3926	42.7	11.6	5.07	7.08
4	16:19	17:19	1.3926	42.3	11.4	5.11	6.97
						average	7.08 (0.09) ^c

^a Concentration in NaOH solution in the first impinger.

^b Calculated from concentration of IO₃⁻ in the solution.

^c Number in parenthesis represents one standard deviation.

S1.3. Specification of the Contactor

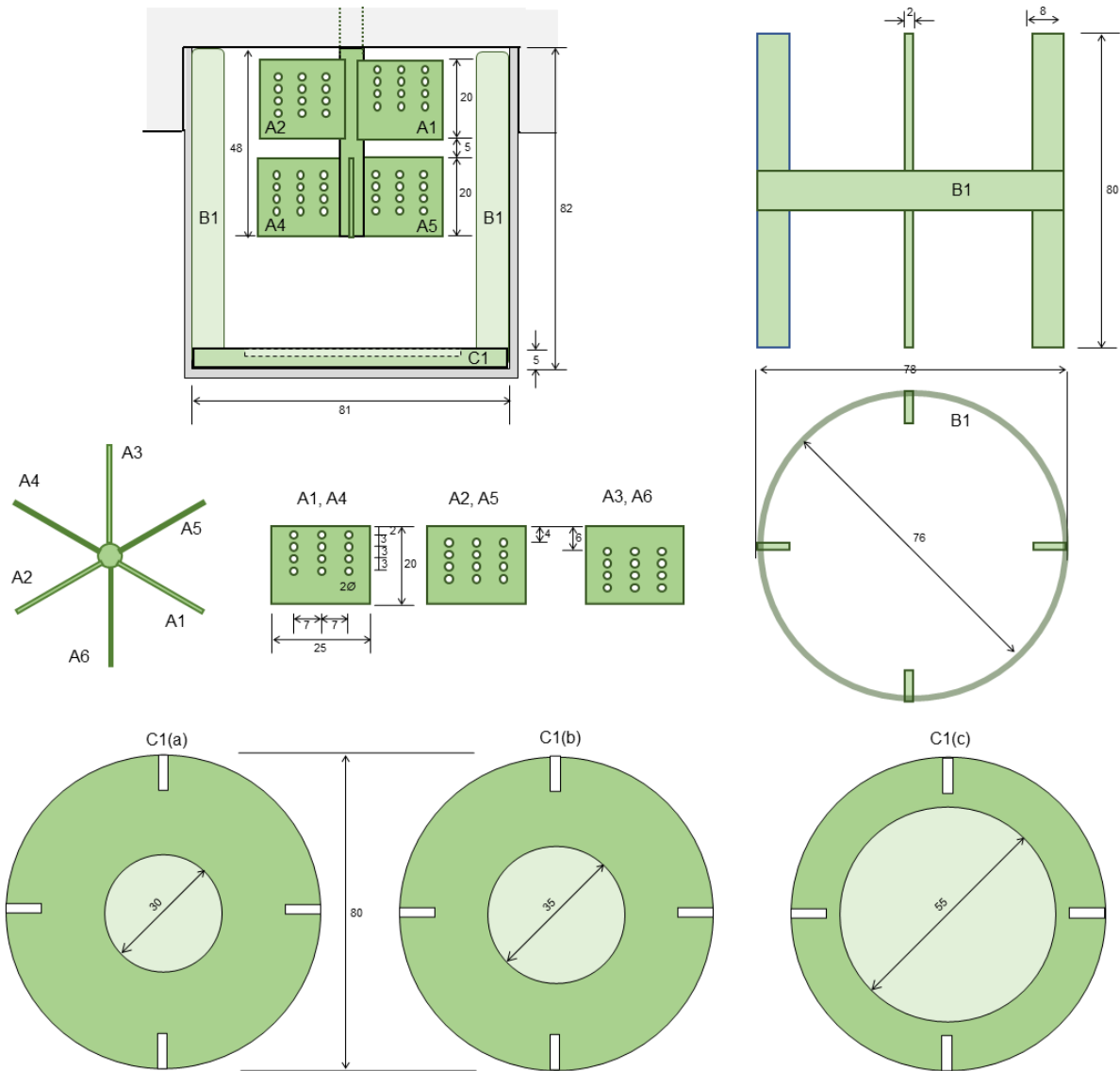


Figure S1. Schematic diagrams of the contactor and details of the PTFE-coated gas-mixing turbine, PTFE-coated stainless-steel baffles, and PTFE dishes with basins. Dimensions are in millimeters. The basin depth is 4 mm for C1(a), 2 mm for C1(b), and 2 or 4 mm for C1(c).

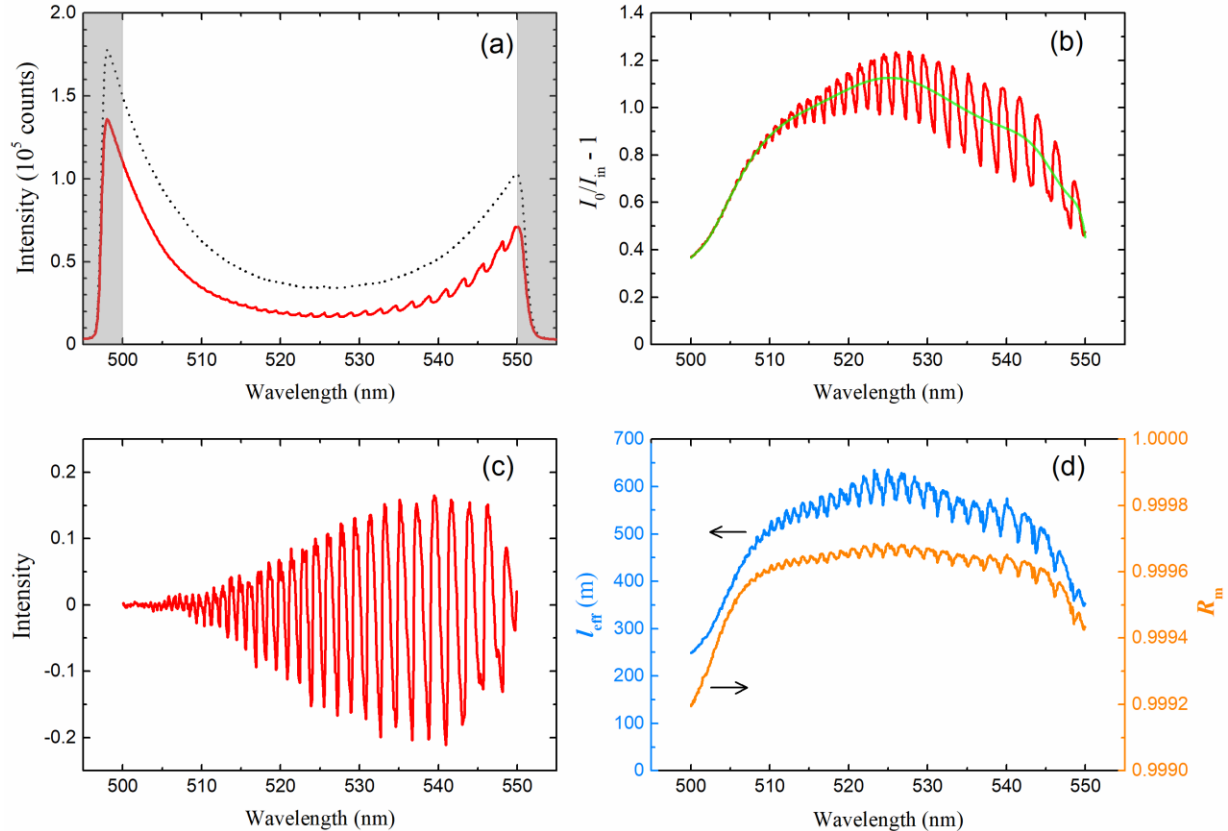
S2. SUPPORTING INFORMATION FOR SECTION 2.3


Figure S2. Examples of measured IBBCEAS spectra of gas mixtures. (a) Transmitted intensity spectrum (I_0) for the CO_2 -air gas mixture (CO_2 , 2.8×10^{-4} atm; gray dashed curve) and spectrum (I_{in}) of I_2 -air(s) (I_2 , 2.8×10^{-7} atm; CO_2 , 2.8×10^{-4} atm; red curve). (b) Spectrum of $(I_0/I_{in} - 1)$ calculated from (a) by eqn (2) (red curve) fitted by a polynomial of order 19 as a smoothing curve (green curve). (c) Residual $(I_0/I_{in} - 1)$ spectrum after subtracting the smoothing curve in (b). (d) Effective pathlength (l_{eff}) in IBBCEAS (blue curve) and mirror reflectivity (R_m) (orange curve), estimated from the IBBCEAS spectrum and the partial pressure of I_2 in I_2 -air(s) determined from ion chromatograph analysis (section 2.2.1).

S3. SUPPORTING INFORMATION FOR SECTION 2.4.2

S3.1. Fitting Rectangular Input Pulse Signals by eqn (13)–(15). The time series of $f_m(t)$ for 0–300 s and 300–1500 s was well reproduced by nonlinear fitting using eqn (13) and (14), respectively (Figure S3).

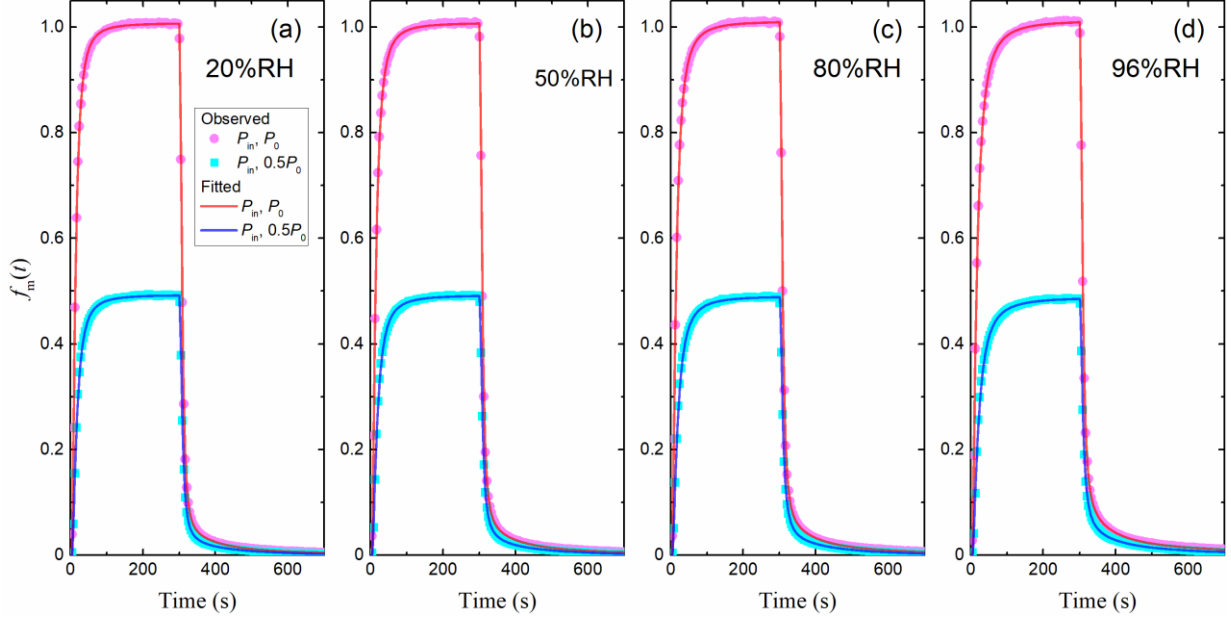


Figure S3. Time series of $f_m(t)$ for P_{in} as P_0 (pink circles) and $0.5P_0$ as P_{in} (blue squares) after the start of injection by the sampling pump at (a) 20% RH, (b) 50% RH, (c) 80% RH, and (d) 96% RH. Curves represent fits to the data by eqn (13) and (14).

The values of parameters a_i and b_i in eqn (13) and (14) thus determined are listed in Table S3.

Table S3. Parameters for eqn (13) and (14)

	Input, P_0				Input, $0.5P_0$			
	20% RH	50% RH	80% RH	96% RH	20% RH	50% RH	80% RH	96% RH
a_1	-0.09411	-0.10269	-0.11810	-0.13714	-0.04586	-0.04943	-0.05277	-0.05258
a_2	1.0075	1.0080	1.0114	1.0132	0.4930	0.4924	0.4907	0.4887
a_3	12.688	13.033	13.130	13.972	16.245	16.845	17.153	18.746
a_4	2.1994	2.1168	2.0001	1.8482	2.1158	2.0336	1.9517	1.8482
b_1	0.74950	0.76558	0.74669	0.78500	0.36919	0.36528	0.44599	0.42292
b_2	9.0331	9.0260	9.1569	9.0146	9.4392	9.5523	8.9424	9.1095
b_3	2.5449	2.4860	2.4818	2.3827	2.4630	2.4449	2.1226	2.1007
b_4	0.1996	0.1727	0.1802	0.1193	0.0768	0.0682	0.0193	0.0356
b_5	0.1677	0.1681	0.1684	0.1707	0.1738	0.1726	0.0126	0.0156
b_6	0.0451	0.0494	0.0565	0.0729	0.0212	0.0287	0.0234	0.0270
b_7	0.0117	0.0132	0.0150	0.0154	0.0228	0.0244	0.0054	0.0040
b_8	0.0123	0.0189	0.0259	0.0320	0.0246	0.0286	0	0
b_9	0.0027	0.0032	0.0037	0.0028	0.0060	0.0060	0	0
$\frac{f_m(300)}{b_1 + b_4 + b_6 + b_8}$	1.0065	1.0066	1.0093	1.0092	0.4918	0.4908	0.4887	0.4855

S4. SUPPORTING INFORMATION FOR SECTION 2.4.3

S4.1. Derivation of eqn (20). Equations (S1)–(S3) apply simultaneously.

$$\frac{dx_m(t)}{dt} = \frac{2}{\tau_m} (x_{out}(t) - x_m(t)) \quad (S1)$$

$$\frac{df_m(t)}{dt} = \frac{2}{\tau_m} (f(t) - f_m(t)) \quad (S2)$$

$$\frac{dP_{out}(t)}{dt} = \frac{1}{\tau_c} \times (P_0 f(t) - P_{out}(t)) - A_{np} U(t) \quad (S3)$$

Because $x_{out}(t) = \frac{P_{out}(t)}{P_0}$ (eqn (7)), eqn (S3) can be rewritten as

$$U(t) = \frac{P_0}{A_{np}} \left(\frac{f(t) - x_{out}(t)}{\tau_c} - \frac{dx_{out}(t)}{dt} \right) \quad (S4)$$

Differentiating eqn (S1) with respect to t gives

$$\frac{dx_{out}(t)}{dt} = \frac{\tau_m}{2} \frac{d^2 x_m(t)}{dt^2} + \frac{dx_m(t)}{dt} \quad (S5)$$

Combining eqn (S1) and (S2) gives

$$f(t) - x_{out}(t) = f_m(t) - x_m(t) + \frac{\tau_m}{2} \left(\frac{df_m(t)}{dt} - \frac{dx_m(t)}{dt} \right) \quad (S6)$$

Substituting eqn (S5) and (S6) into eqn (S4) yields eqn (S7), that is, eqn (20).

$$U(t) = \frac{P_0}{A_{np}} \times \left(\frac{f_m(t) - x_m(t)}{\tau_c} - \frac{\tau_m}{2\tau_c} \frac{dx_m(t)}{dt} + \frac{\tau_m}{2\tau_c} \frac{df_m(t)}{dt} - \frac{\tau_m}{2} \frac{d^2 x_m(t)}{dt^2} - \frac{dx_m(t)}{dt} \right) \quad (S7)$$

S5. SUPPORTING INFORMATION FOR SECTION 3.1

S5.1. I₂ Loss Rates in Blank Experiments

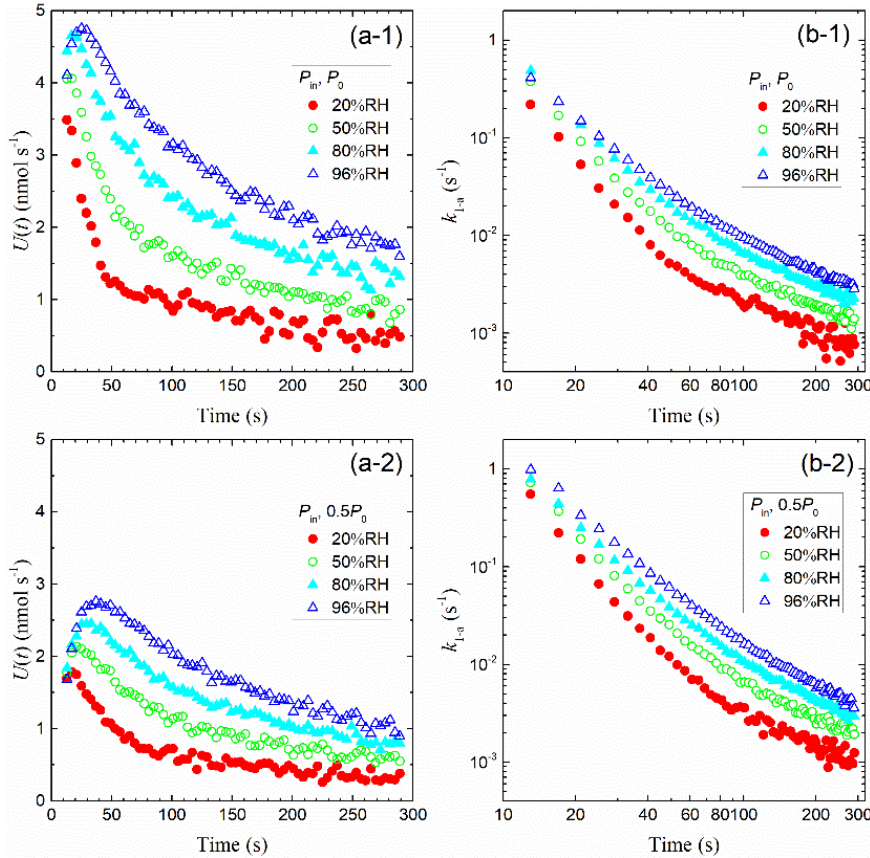


Figure S4. Time series of (a) loss rates of I₂ by uptake, $U(t)$ (eqn (20)), and (b) their apparent first-order rate constants, $k_{1-a}(t)$ (eqn (21)), at 20% RH, 50% RH, 80% RH, and 96% RH calculated from data (Figure 3) in blank experiments (1) with P_0 as P_{in} and (2) with $0.5P_0$ as P_{in} .

S5.2. Freundlich-type and Langmuir-type Adsorption Equilibria. Table S4 lists the parameters and the loss ratios determined by the simulation with eqn (12) and eqn (26)–(28) under the assumption of Freundlich-type adsorption equilibrium ($N = 2$) of I₂ on the contactor wall.

When Langmuir-type adsorption of I₂ on the contactor wall was assumed, eqn (S8)–(S10) were used instead of eqn (26)–(28).

$$\frac{dx_{out}(t)}{dt} = \frac{1}{\tau_c} \times (f(t) - x_{out}(t)) - k_{bml} \times \left(x_{out}(t) - \frac{\theta_b(t)}{1-\theta_b(t)} \frac{1}{K_{badsl}} \right) \quad (S8)$$

$$\frac{d\theta_b(t)}{dt} = \frac{A_{pnl}}{q_{b\infty}} \left(x_{out}(t) - \frac{\theta_b(t)}{1-\theta_b(t)} \frac{1}{K_{badsl}} \right) - k_{bfl}\theta_b(t) + k_{bbl}\varphi_b(t) \quad (S9)$$

$$\frac{d\varphi_b(t)}{dt} = k_{bfl}\theta_b(t) - k_{bbl}\varphi_b(t) - k_{bll}\varphi_b(t) \quad (S10)$$

where k_{bml} is the mass-transfer coefficients of I₂ between the gas-phase and the wall surface; K_{badsl} is the adsorption equilibrium constant of I₂ on the wall surface; k_{bfl} and k_{bbl} are first-order forward and backward rate constants, respectively, for reversible transformation of adsorbents between surface and interior sites of the wall; k_{bll} is the

first-order rate constant for loss of I₂ in interior sites; q_{bt} and $q_{b\infty}$ denote the amount of I₂ adsorbed at time t and when the wall surface is fully saturated, respectively, and $\theta_b(t)$ is the fractional coverage of the contactor wall surface, that is, $q_{bt}/q_{b\infty}$; $\varphi_b(t)$ is the number of interior sites into which I₂ has been transformed as a fraction of $q_{b\infty}$; and A_{pn1} is a conversion factor of units. Simulations using eqn (12) and eqn (S8)–(S10) were conducted to simultaneously reproduce time series of observed $x_m(t)$ in both the cases of P_0 and $0.5P_0$ as P_{in} for four RH values with values of $q_{b\infty}$, K_{badsl} , k_{bfl} , k_{bb} , and k_{bl} as common parameters while the value of k_{bml} was assumed at 0.5 s⁻¹; the results are listed in Table S5. This simulation yielded much larger RSS errors than those in Table S4.

Table S4. Parameters Optimized to Reproduce the Time Series of $x_m(t)$ in Blank Experiments with eqn (12) and eqn (26)–(28) and Freundlich-type Adsorption Equilibrium

	20% RH	50% RH	80% RH	96% RH
<i>n</i>	2 (fixed)			
k_{bm} (s ⁻¹)	0.6593 (This parameter is common at 20–96 %RH)			
K_{badsl} (nmol atm ^{-0.5})	1.485	2.300	3.051	3.710
k_{bf} (10 ⁻³ s ⁻¹)	5.128	6.993	8.594	9.727
k_{bb} (10 ⁻³ s ⁻¹)	2.335	3.698	4.773	4.593
k_{bl} (10 ⁻³ s ⁻¹)	0.152	0.811	1.018	1.193
loss ratio (%)	$P_{in} = P_0$	2.7	5.6	8.3
	$P_{in} = 0.5P_0$	2.2	6.5	10.2
RSS	72.6	71.3	44.7	190.8

Table S5. Parameters Optimized to Reproduce the Time Series of $x_m(t)$ in Blank Experiments with eqn (12) and eqn (S8)–(S10) and Langmuir-type Adsorption Equilibrium

	20% RH	50% RH	80% RH	96% RH
k_{bml} (s ⁻¹)	0.5 (fixed)			
$q_{b\infty}$ (nmol)	2.049	3.302	5.206	6.080
K_{badsl} (nmol atm ⁻¹)	2.487	2.353	1.829	2.005
k_{bfl} (10 ⁻³ s ⁻¹)	3.994	4.614	4.870	6.111
k_{bb} (10 ⁻³ s ⁻¹)	1.125	1.777	1.794	2.515
k_{bl} (10 ⁻³ s ⁻¹)	0.378	0.937	1.120	1.738
loss ratio (%)	$P_{in} = P_0$	2.7	4.9	7.8
	$P_{in} = 0.5P_0$	3.8	6.8	10.3
RSS	251.2	273.2	354.5	675.5

S6. SUPPORTING INFORMATION FOR SECTION 3.2

S6.1. Estimated Dissociation Ratios in Relation R1 under Experimental Conditions. Equation (29) is derived from reaction R1. Under the experimental conditions, water is in equilibrium with 400 ppmv CO₂ in I₂-air(s) and thus has a pH of about 5.6 at 283 K. Literature values of K_a and K_H at 283 K are 1.2×10^{-13} M²² and 6.0 M atm⁻¹, respectively. Substituting these values plus $P_{I_2} = 3.2 \times 10^{-7}$ atm and $[H^+] = 10^{-5.6}$ M into eqn (29) gives $[HOI]/[I_2] = [I^-]/[I_2] = 0.16$.

S6.2. Apparent Surface Resistance for I₂ above Aqueous Surfaces.

Table S6. Values of k_{1-a} , k_{g-a} , and R_{g-a} for Runs 1 and 2 above Aqueous Solutions

sample	$x_{out}(t)$ ^a	$10^2 k_{1-a} (\text{s}^{-1})$ ^a			k_{g-a} (cm s ⁻¹)	R_{g-a} (s m ⁻¹)
		From eqn (21)	After blank correction	P_{in} for blank		
blank	$P_{in} = P_0$	0.820 ± 0.008	0.32 ± 0.02			
	$P_{in} = 0.5P_0$	0.369 ± 0.006	0.42 ± 0.04			
S/S _c	run no.					
10 mM ascorbic acid	0.138	1	0.471 ± 0.002	2.00 ± 0.04	1.67 ± 0.05 1.58 ± 0.06	P_0 $0.5P_0$ 0.86 ± 0.03 116 ± 5
		2	0.489 ± 0.003	1.85 ± 0.03	1.53 ± 0.03 1.43 ± 0.05	P_0 $0.5P_0$ 0.83 ± 0.02 120 ± 3
	0.461	1	0.243 ± 0.003	5.55 ± 0.07	5.22 ± 0.07 5.13 ± 0.08	P_0 $0.5P_0$ 0.85 ± 0.01 118 ± 2
		2	0.246 ± 0.003	5.45 ± 0.10	5.12 ± 0.10 5.03 ± 0.10	P_0 $0.5P_0$ 0.83 ± 0.02 120 ± 2
1 mM ascorbic acid	0.138	1	0.475 ± 0.003	1.95 ± 0.05	1.63 ± 0.05 1.53 ± 0.06	P_0 $0.5P_0$ 0.89 ± 0.03 113 ± 3
		2	0.487 ± 0.002	1.87 ± 0.05	1.55 ± 0.06 1.45 ± 0.07	P_0 $0.5P_0$ 0.85 ± 0.03 118 ± 4
	0.461	1	0.246 ± 0.002	5.45 ± 0.06	5.13 ± 0.06 5.03 ± 0.07	P_0 $0.5P_0$ 0.83 ± 0.01 120 ± 1
		2	0.250 ± 0.003	5.33 ± 0.10	5.00 ± 0.10 4.91 ± 0.11	P_0 $0.5P_0$ 0.82 ± 0.01 122 ± 2
water	0.138	1	0.774 ± 0.007	0.46 ± 0.03	0.14 ± 0.03	P_0 0.08 ± 0.02 1300 ± 300
		2	0.778 ± 0.020	0.44 ± 0.03	0.12 ± 0.04	P_0 0.06 ± 0.02 1600 ± 600
	0.461	1	0.524 ± 0.010	1.49 ± 0.05	1.16 ± 0.06	P_0 0.19 ± 0.01 580 ± 40
		2	0.563 ± 0.012	1.22 ± 0.06	0.90 ± 0.06	P_0 0.15 ± 0.01 690 ± 50
1 mM sulfuric acid	0.138	1	0.774 ± 0.009	0.46 ± 0.03	0.12 ± 0.04	P_0 0.07 ± 0.02 1400 ± 300
	2		0.779 ± 0.010	0.42 ± 0.04	0.10 ± 0.05	P_0 0.05 ± 0.03 3400 ± 2100

^a Each value is the average of 10 data points from 253–289 s.

S6.3. Simulation of uptake of I₂ above Aqueous Ascorbic Acid.

Simulations were carried out to distinguish the uptake of I₂ by ascorbic acid and the contactor. Because the mass transfer in the gas-film layer is the rate-limiting step in I₂ uptake above aqueous ascorbic acid, on the basis of eqn (26) we assumed

$$\frac{dx_{\text{out}}(t)}{dt} = \frac{1}{\tau_c} \times (f(t) - x_{\text{out}}(t)) - \frac{s}{s_c h_c} k_m \times x_{\text{out}}(t) - k_{\text{bm}} \times \left\{ x_{\text{out}}(t) - \left(\frac{y_b(t)}{K_{\text{bad}}} \right)^2 \right\} \quad (\text{S11})$$

where k_m is the mass-transfer coefficient of I_2 in the gas-film layer above ascorbic acid. Simulations using eqn (12), (27), (28), and (S11) were conducted to reproduce time series of $x_m(t)$. Although the simulation with the small basin successfully reproduced the time series of $x_m(t)$ with $k_m = 0.91 \text{ cm s}^{-1}$, the simulation with the large basin never reproduced the data. We assumed additional Freundlich-type adsorption of I_2 onto the contactor for the large-basin case and performed the simulation with

$$\begin{aligned} \frac{dx_{\text{out}}(t)}{dt} &= \frac{1}{\tau_c} \times (f(t) - x_{\text{out}}(t)) - \frac{s}{s_c h_c} k_m \times x_{\text{out}}(t) - k_{\text{bm}} \times \left\{ x_{\text{out}}(t) - \left(\frac{y_b(t)}{K_{\text{bad}}} \right)^2 \right\} \\ &\quad - k_{\text{bma}} \times \left\{ x_{\text{out}}(t) - \left(\frac{y_{\text{ba}}(t)}{K_{\text{bad}}} \right)^2 \right\} \end{aligned} \quad (\text{S12})$$

$$\frac{dy_{\text{ba}}(t)}{dt} = A_{\text{bpn}} k_{\text{bma}} \times \left\{ x_{\text{out}}(t) - \left(\frac{y_{\text{ba}}(t)}{K_{\text{bad}}} \right)^2 \right\} \quad (\text{S13})$$

where k_{bma} is the mass-transfer coefficient of I_2 for additional adsorption between gas and the contactor (determined as 0.0481), K_{bad} is the corresponding parameter of Freundlich adsorption equilibrium (determined as 1.38), and $y_{\text{ba}}(t)$ is the additional amount of I_2 adsorbed onto the contactor. Figure 4 shows the obtained values of $x_m(t)$ as solid curves. Values of k_m are thus estimated at $0.91 \pm 0.01 \text{ cm s}^{-1}$ and $0.78 \pm 0.01 \text{ cm s}^{-1}$ for the small and large basins, respectively (errors at 90% confidence level).

S6.4. Estimate of Uptake Coefficient (γ) of I_2 on Ascorbic Acid.

Values of γ were derived from

$$\frac{1}{\gamma} = \frac{1}{\alpha} + \frac{v_m}{4HRT \sqrt{D_l k \left(\text{erf}(\sqrt{kt}) + \frac{e^{-kt}}{\sqrt{\pi kt}} \right)}} \quad (\text{S14})$$

where α is the accommodation coefficient, v_m is the molecular velocity in cm s^{-1} , H is the Henry's law constant in M atm^{-1} as obtained below, R is the gas constant ($0.0821 \text{ M}^{-1} \text{ atm K}^{-1}$), T is the temperature in K, D_l is the diffusion constant in the liquid phase in $\text{cm}^2 \text{ s}^{-1}$ as obtained below, k is the pseudo-first-order rate constant in the aqueous phase as obtained below, and t is the time during which gas is exposed to the aqueous surface. k is obtained by

$$k = k_{\text{R3}}[\text{ASC}] \quad (\text{S15})$$

where k_{R3} is a rate constant in $\text{M}^{-1} \text{ s}^{-1}$ for reaction R3, and $[\text{ASC}]$ is the aqueous concentration of ascorbic acid in M. Under the experimental conditions for 10 mM ascorbic acid ($kt \gg 1$), eqn (S14) is approximated by

$$\frac{1}{\gamma} = \frac{1}{\alpha} + \frac{v_m}{4HRT \sqrt{D_l k_{\text{R3}}[\text{ASC}]}} \quad (\text{S16})$$

HRT is obtained from⁴

$$\ln(HRT) = 2.8 \times \exp \left[4300 \times \left(\frac{1}{T} - \frac{1}{298.2} \right) \right] \quad (\text{S17})$$

and D_l is obtained from⁵

$$D_l = \frac{7.4 \times 10^{-8} (\phi M_B)^{1/2} T}{\eta_B V_A^{0.6}} \quad (\text{S18})$$

where ϕ is the dimensionless association factor of water (2.6), M_B is the molecular weight of water (18 g mol⁻¹), η_B is the viscosity of water (1.3064 cP at 283 K), and V_A is the molar volume of I₂ in cm² mol⁻¹ at its normal boiling temperature, estimated at 77 cm² mol⁻¹ by additive methods. Thus D_l is calculated to be 8.09×10^{-6} cm² s⁻¹ at 283 K. Substituting $\alpha = 10^{-2}$, $v_m = 1.54 \times 10^4$, $H = 6.0$, $T = 283$, and $D_l = 8.09 \times 10^{-6}$ into eqn (S16) gives

$$\frac{1}{\gamma} = 100 + \frac{9710}{\sqrt{k_{R3}[\text{ASC}]}} \quad (\text{S19})$$

The value of k_{R3} reported at 293 K (1.2×10^5 M⁻¹ s⁻¹)⁷ is used to estimate γ by eqn (S19), yielding $\gamma = 2.6 \times 10^{-3}$ for 10 mM ascorbic acid and 1.0×10^{-3} for 1 mM ascorbic acid. If there is no resistance against the gas-film transfer, γ values are related to k_m values by

$$k_m = \frac{1}{4} \gamma v_m \quad (\text{S20})$$

Because v_m is 1.54×10^4 cm s⁻¹ at 283 K, the γ values of 2.6×10^{-3} and 1.0×10^{-3} would correspond to mass-transfer coefficients of 10.0 cm s⁻¹ and 3.9 cm s⁻¹, that is, surface resistance of 10 s m⁻¹ and 26 s m⁻¹, respectively, in the absence of gas-film transfer resistance.

S7. SUPPORTING INFORMATION FOR SECTION 3.3

S7.1. Time Series of I₂ in I₂–air(s) Flowing over Clay Samples.

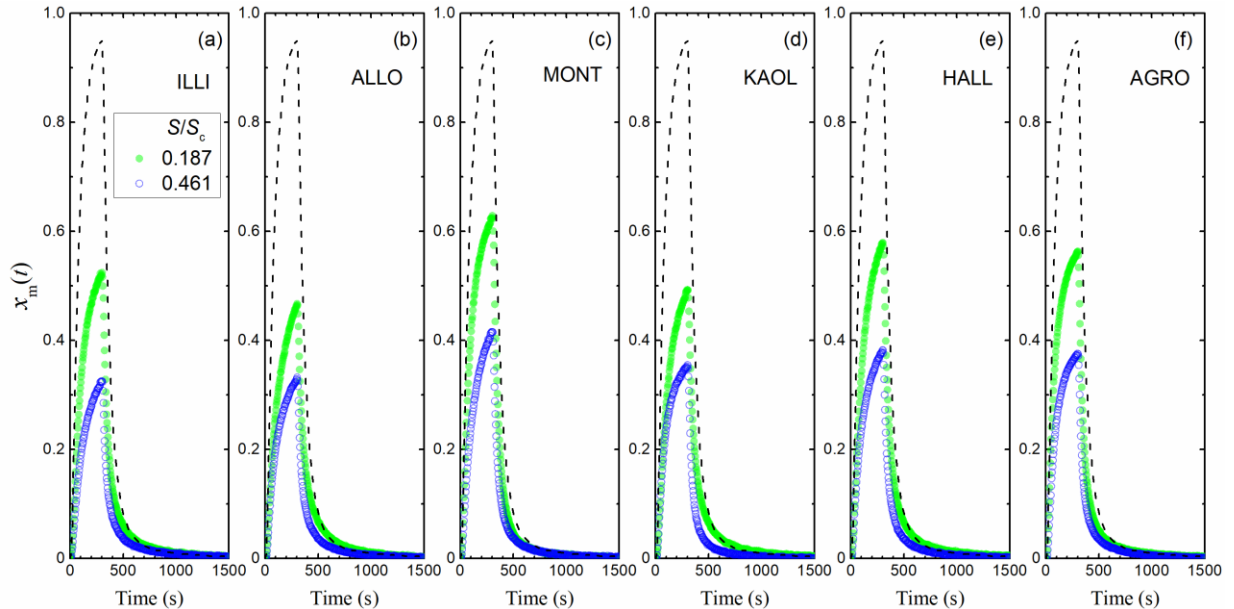


Figure S5. Time series of $x_m(t)$ in I₂–air(s) leaving the contactor (P_0 , 4.0×10^{-7} atm) at 20% RH after flowing over clay samples in run 1. Other experimental conditions were the same as those at 80% RH (Figure 6).

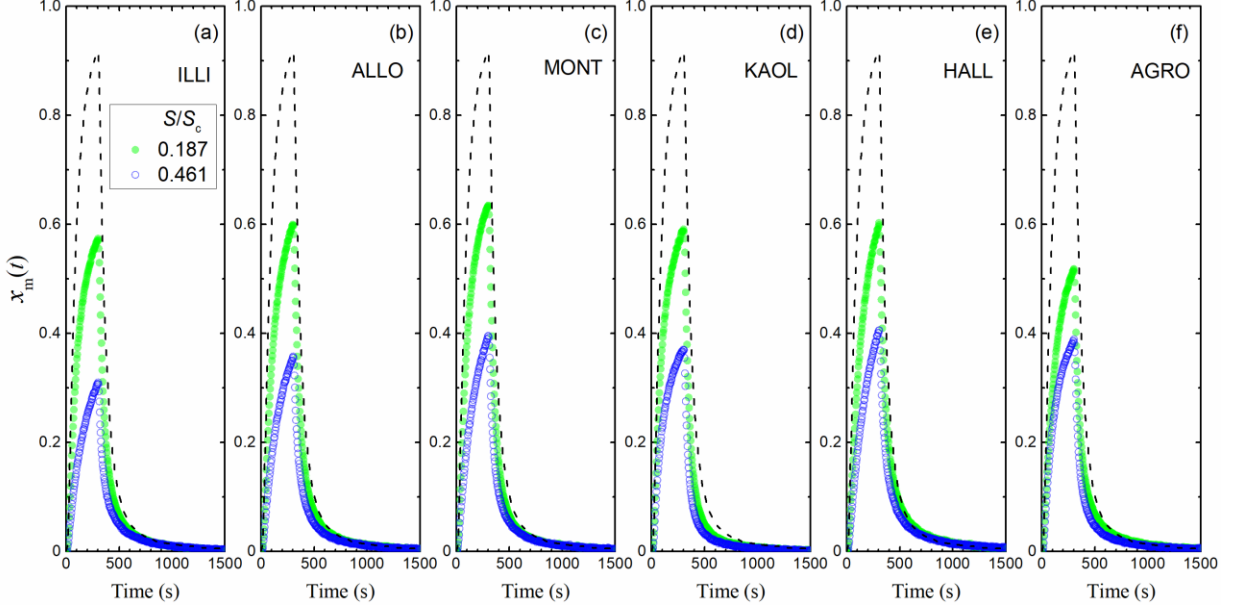


Figure S6. Same as Figure S5, for 50% RH.

S7.2. Ratios of $\Delta Q_{\text{loss}}/Q_{\text{in}}$ and $\Delta Q_{\text{ads}}/Q_{\text{in}}$ in Different Runs at 20% RH, 50% RH, and 80% RH.

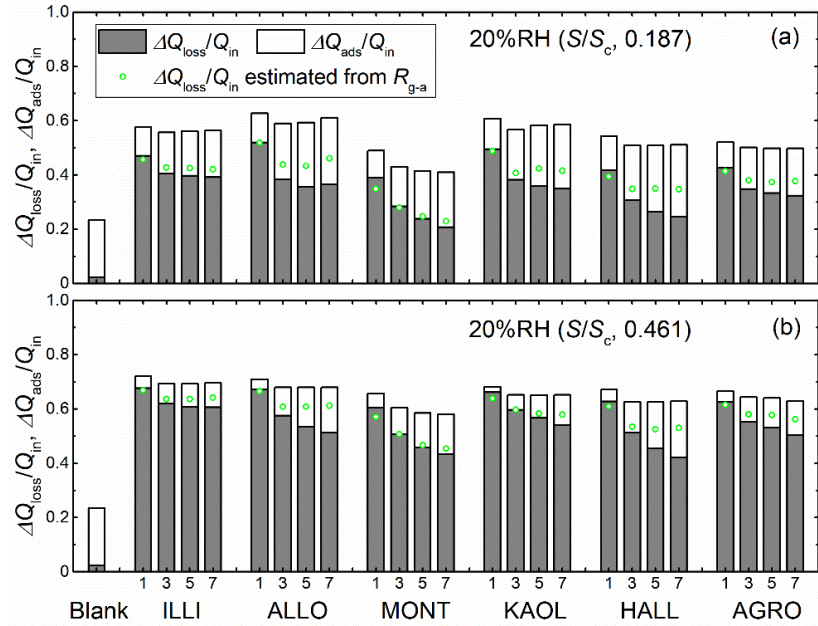


Figure S7. Ratios of $\Delta Q_{\text{loss}}/Q_{\text{in}}$ and $\Delta Q_{\text{ads}}/Q_{\text{in}}$ in odd-numbered runs ($P_{\text{in}}, 4.0 \times 10^{-7} \text{ atm}$) for clay samples at 20% RH for experiments with (a) the small basin ($S/S_c, 0.187$) and (b) the large basin ($S/S_c, 0.461$). Green circle symbols represent $\Delta Q_{\text{loss}}/Q_{\text{in}}$ estimated from R_{g-a} (Tables S8–S13) using eqn (S21). See the text (section S7.3) for explanation.

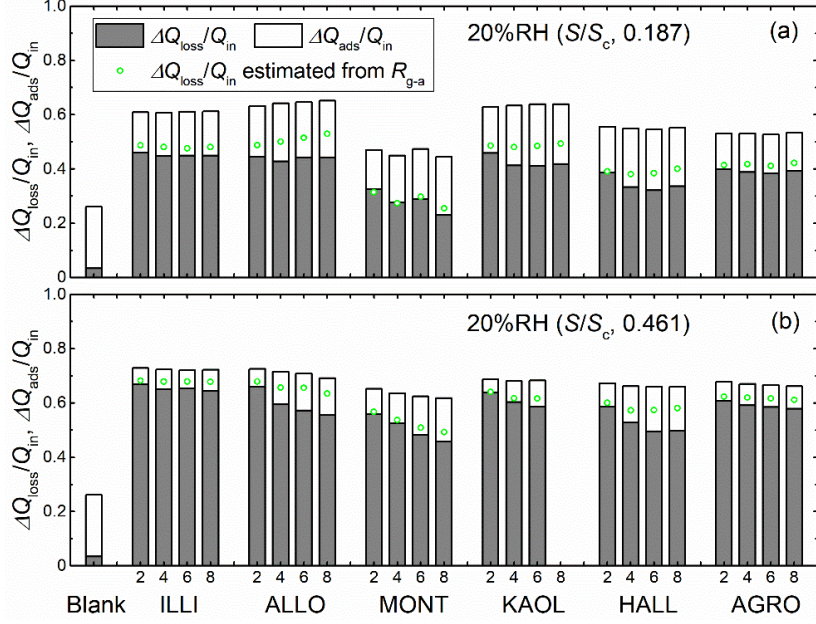


Figure S8. Same as Figure S7, but in even-numbered runs ($P_{\text{in}}, 2.0 \times 10^{-7} \text{ atm}$) for 20% RH. Data for run 8 for kaolinite with the large basin are missing because I_2 -air(s) was not introduced into the contactor.

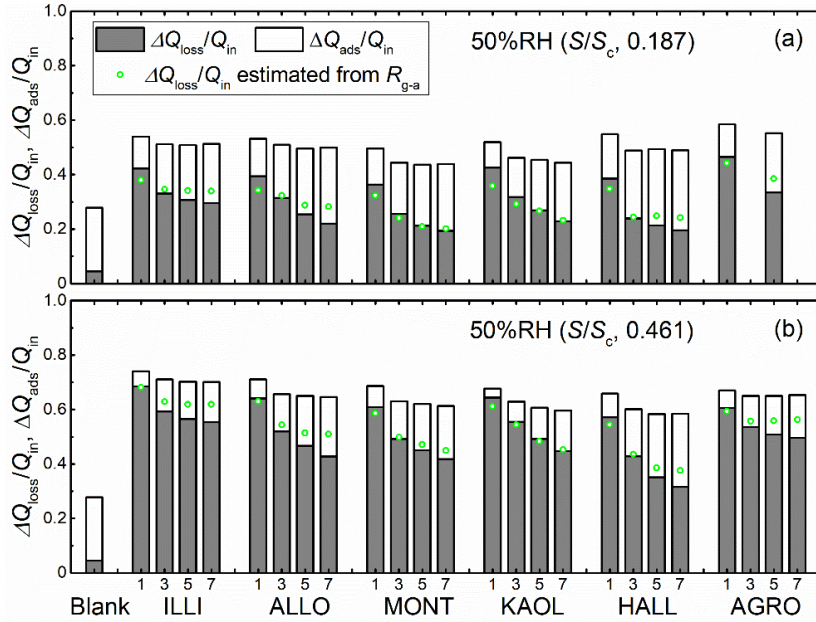


Figure S9. Same as Figure S7, but in odd-numbered runs ($P_{\text{in}}, 4.0 \times 10^{-7} \text{ atm}$) for 50% RH. Data for run 3 and run 7 for AgroMAT AG-1 with the small basin are missing because the baseline was changed during run 3 and because I_2 -air(s) was not introduced into the contactor in run 7.

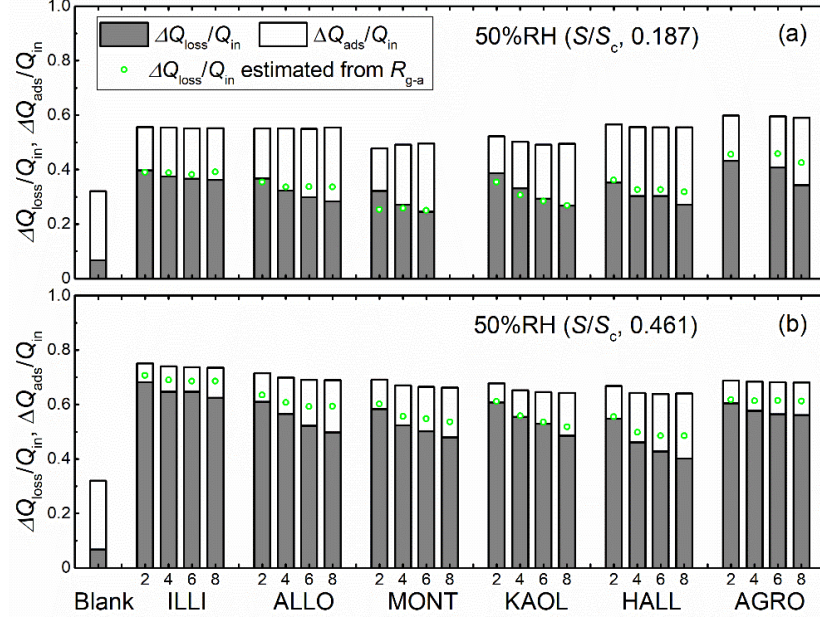


Figure S10. Same as Figure S7, but in even-numbered runs ($P_{\text{in}}, 2.0 \times 10^{-7} \text{ atm}$) for 50% RH. Data for run 4 for AgroMAT AG-1 with the small basin are missing because the baseline was changed during the run.

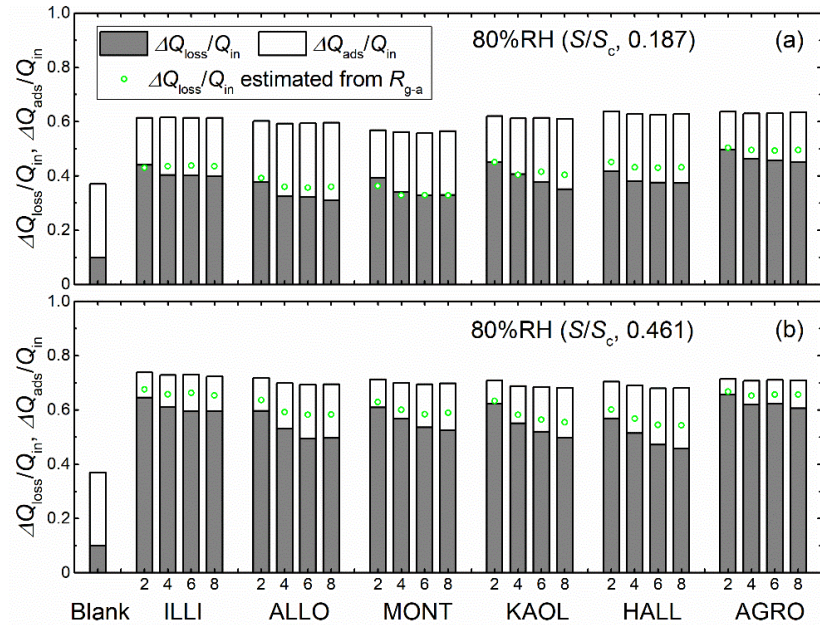


Figure S11. Same as Figure S7, but in even-numbered runs ($P_{\text{in}}, 2.0 \times 10^{-7} \text{ atm}$) for 80% RH.

S7.3. Apparent Surface Resistance for I₂ above Clay Samples. We used a procedure analogous to our procedure for the aqueous solutions (section 3.2) to obtain the values of k_{1-a} , k_{g-a} , and R_{g-a} from 10 values of $k_{1-a}(t)$ at times of 253–289 s. Values of k_{1-a} in blank experiments in which values of P_0 or $0.5P_0$ were used as P_{in} at each value of RH (Table S7) were used to calculate k_{1-a} values for the clay samples (Tables S8–S13).

Table S7. Values of k_{1-a} in Blank Experiments

RH	P_{in}	$x_{out}(t)$ ^a	$10^2 k_{1-a} (\text{s}^{-1})$ ^a
20	P_0	0.943	0.08 ± 0.02
	$0.5P_0$	0.450	0.11 ± 0.02
50	P_0	0.904	0.14 ± 0.02
	$0.5P_0$	0.422	0.22 ± 0.02
80	P_0	0.861	0.23 ± 0.02
	$0.5P_0$	0.396	0.30 ± 0.02

^a Each value is the average of 10 data points from 253–289 s. Uncertainties (\pm) are standard deviations.

As shown in Figure 10, uptake of I₂ decreased with time after about 50 s, although the gas-phase concentration of I₂ increased. Values of $k_{1-a}(t)$ and $k_{g-a}(t)$ decreased by an order of magnitude or more. The similarity of the decrease we observed for all clay samples suggested that there was a non-linear relationship between the I₂ uptake rates and gaseous concentrations of I₂.

$R_{g-a}(t)$ increased with time during the injection period, but if surface resistance were a constant value equal to R_{gc} , then $\Delta Q_{loss}/Q_{in}$ would be given by (see section S7.4)

$$\frac{\Delta Q_{loss}}{Q_{in}} = \frac{1}{1 + \frac{T_0 F_g}{T S} R_{gc}} \quad (\text{S21})$$

Figure 9 and S7–S11 show the values of $\Delta Q_{loss}/Q_{in}$ calculated with eqn (S21) and assuming $R_{gc} = R_{g-a}$. The calculated values agreed with the observed values within an error range of 30%, except for two runs (run 5 and run 7 for halloysite with the small basins at 20%RH). Values of R_{g-a} thus represent the surface resistance for I₂ above the clay samples.

S7.4. Derivation of eqn (S21). Let $q_{out}(t)$ and $q_{loss}(t)$ be rates for I₂ leaving the contactor and I₂ loss, respectively, at time t . Their ratios are given by

$$\frac{q_{loss}(t)}{q_{out}(t)} = \frac{S k_g(t)}{F_g \times \frac{T}{T_0}} = \frac{T_0}{T} \frac{S}{F_g} \frac{1}{R_g(t)} \quad (\text{S22})$$

Because $\Delta Q_{loss} = \int_0^{t_m} q_{loss}(t) dt$ where t_m was 1709 s, eqn (S22) was rewritten as

$$\Delta Q_{loss} = \frac{T_0}{T} \frac{S}{F_g} \int_0^{t_m} \frac{q_{out}(t)}{R_g(t)} dt \quad (\text{S23})$$

The value of $R_g(t)$ increased with time during the injection period, but if $R_g(t)$ were a constant value equal to R_{gc} , eqn (S21) would be given from eqn (S23) and $\int_0^{t_m} q_{out}(t) dt = Q_{out} = Q_{in} - \Delta Q_{loss}$.

Table S8. Values of k_{1-a} , k_{g-a} , and R_{g-a} for Successive Runs with Illite Sample

RH (%)	P_{in}	Run	S/S_c	$x_{out}(t)$ ^a	$10^2 k_{1-a} (\text{s}^{-1})$ ^a		k_{g-a} (cm s^{-1})	$R_{g-a} (\text{s m}^{-1})$	
					From eqn (21)	After blank correction		value	average
20	P_0	1	0.187	0.514	1.629	1.520	$0.5P_0$	0.61 ± 0.02	164 ± 6
			0.461	0.317	3.752	3.643	$0.5P_0$	0.59 ± 0.02	169 ± 5
		3	0.187	0.541	1.457	1.349	$0.5P_0$	0.54 ± 0.02	185 ± 8
			0.461	0.348	3.284	3.175	$0.5P_0$	0.52 ± 0.01	194 ± 3
		5	0.187	0.542	1.445	1.336	$0.5P_0$	0.54 ± 0.02	186 ± 7
			0.461	0.349	3.276	3.167	$0.5P_0$	0.52 ± 0.01	194 ± 4
		7	0.187	0.542	1.423	1.314	$0.5P_0$	0.53 ± 0.02	189 ± 7
			0.461	0.344	3.357	3.248	$0.5P_0$	0.53 ± 0.01	189 ± 3
	$0.5P_0$	2	0.187	0.237	1.824	1.715	$0.5P_0$	0.69 ± 0.04	145 ± 8
			0.461	0.147	3.997	3.888	$0.5P_0$	0.63 ± 0.02	158 ± 4
		4	0.187	0.238	1.780	1.672	$0.5P_0$	0.67 ± 0.02	149 ± 5
			0.461	0.150	3.944	3.835	$0.5P_0$	0.62 ± 0.02	160 ± 5
		6	0.187	0.238	1.758	1.649	$0.5P_0$	0.66 ± 0.03	151 ± 8
			0.461	0.150	3.928	3.819	$0.5P_0$	0.62 ± 0.02	161 ± 6
		8	0.187	0.237	1.785	1.676	$0.5P_0$	0.67 ± 0.03	149 ± 7
			0.461	0.150	3.918	3.809	$0.5P_0$	0.62 ± 0.02	161 ± 4
50	P_0	1	0.187	0.561	1.322	1.103	$0.5P_0$	0.44 ± 0.02	226 ± 11
			0.461	0.297	4.075	3.857	$0.5P_0$	0.63 ± 0.02	159 ± 6
		3	0.187	0.602	1.094	0.951	P_0	0.38 ± 0.02	262 ± 11
			0.461	0.343	3.259	3.041	$0.5P_0$	0.49 ± 0.01	202 ± 5
		5	0.187	0.604	1.075	0.932	P_0	0.37 ± 0.02	267 ± 13
			0.461	0.351	3.144	2.925	$0.5P_0$	0.48 ± 0.02	210 ± 7
		7	0.187	0.605	1.069	0.926	P_0	0.37 ± 0.02	269 ± 15
			0.461	0.352	3.145	2.926	$0.5P_0$	0.48 ± 0.01	210 ± 6
	$0.5P_0$	2	0.187	0.267	1.370	1.151	$0.5P_0$	0.46 ± 0.02	216 ± 7
			0.461	0.133	4.576	4.357	$0.5P_0$	0.71 ± 0.03	141 ± 6
		4	0.187	0.267	1.360	1.141	$0.5P_0$	0.46 ± 0.02	218 ± 8
			0.461	0.140	4.229	4.011	$0.5P_0$	0.65 ± 0.03	153 ± 7
		6	0.187	0.268	1.333	1.114	$0.5P_0$	0.45 ± 0.03	223 ± 13
			0.461	0.141	4.156	3.938	$0.5P_0$	0.64 ± 0.02	156 ± 5
		8	0.187	0.265	1.376	1.157	$0.5P_0$	0.46 ± 0.03	215 ± 13
			0.461	0.143	4.142	3.923	$0.5P_0$	0.64 ± 0.02	157 ± 6
80	P_0	1	0.187	0.533	1.460	1.156	$0.5P_0$	0.46 ± 0.02	215 ± 10
			0.461	0.326	3.548	3.243	$0.5P_0$	0.53 ± 0.02	190 ± 7
		3	0.187	0.558	1.297	0.993	$0.5P_0$	0.40 ± 0.03	251 ± 17
			0.461	0.372	2.872	2.568	$0.5P_0$	0.42 ± 0.02	239 ± 9
		5	0.187	0.579	1.185	0.880	$0.5P_0$	0.35 ± 0.02	283 ± 14
			0.461	0.377	2.803	2.499	$0.5P_0$	0.41 ± 0.02	246 ± 10
		7	0.187	0.576	1.200	0.895	$0.5P_0$	0.36 ± 0.03	278 ± 22
			0.461	0.393	2.602	2.298	$0.5P_0$	0.37 ± 0.01	268 ± 9
	$0.5P_0$	2	0.187	0.239	1.671	1.367	$0.5P_0$	0.55 ± 0.03	182 ± 10
			0.461	0.143	4.073	3.769	$0.5P_0$	0.61 ± 0.02	163 ± 6
		4	0.187	0.238	1.680	1.375	$0.5P_0$	0.55 ± 0.04	181 ± 14
			0.461	0.150	3.785	3.481	$0.5P_0$	0.57 ± 0.03	177 ± 9
		6	0.187	0.237	1.712	1.408	$0.5P_0$	0.57 ± 0.02	177 ± 7
			0.461	0.148	3.860	3.556	$0.5P_0$	0.58 ± 0.02	173 ± 7
		8	0.187	0.237	1.698	1.393	$0.5P_0$	0.56 ± 0.02	179 ± 7
			0.461	0.153	3.713	3.408	$0.5P_0$	0.55 ± 0.03	180 ± 9

^a Each value is the average of 10 data points from 253–289 s. Errors are standard deviations.

Table S9. Values of k_{1-a} , k_{g-a} , and R_{g-a} for Successive Runs with Allophane Sample

RH (%)	P_{in}	Run	S/S_c	$x_{out}(t)$ ^a	$10^2 k_{1-a} (\text{s}^{-1})$ ^a		k_{g-a} (cm s^{-1})	$R_{g-a} (\text{s m}^{-1})$	
					From eqn (21)	After blank correction		value	average
20	P_0	1	0.187	0.452	2.062	1.954	$0.5P_0$	0.78 ± 0.03	127 ± 4
			0.461	0.321	3.703	3.594	$0.5P_0$	0.58 ± 0.01	171 ± 4
		3	0.187	0.523	1.520	1.411	$0.5P_0$	0.57 ± 0.03	176 ± 9
			0.461	0.372	2.919	2.810	$0.5P_0$	0.46 ± 0.01	219 ± 6
		5	0.187	0.526	1.493	1.384	$0.5P_0$	0.57 ± 0.02	180 ± 8
			0.461	0.372	2.921	2.813	$0.5P_0$	0.46 ± 0.01	219 ± 6
		7	0.187	0.502	1.658	1.549	$0.5P_0$	0.62 ± 0.03	161 ± 7
			0.461	0.370	2.966	2.857	$0.5P_0$	0.46 ± 0.01	215 ± 5
	$0.5P_0$	2	0.187	0.231	1.836	1.727	$0.5P_0$	0.69 ± 0.03	144 ± 6
			0.461	0.149	3.928	3.819	$0.5P_0$	0.62 ± 0.03	161 ± 7
		4	0.187	0.225	1.920	1.812	$0.5P_0$	0.73 ± 0.04	137 ± 7
			0.461	0.159	3.572	3.463	$0.5P_0$	0.56 ± 0.02	178 ± 7
		6	0.187	0.220	2.026	1.918	$0.5P_0$	0.77 ± 0.03	130 ± 5
			0.461	0.160	3.550	3.441	$0.5P_0$	0.56 ± 0.02	179 ± 5
		8	0.187	0.214	2.142	2.033	$0.5P_0$	0.82 ± 0.03	122 ± 4
			0.461	0.169	3.255	3.146	$0.5P_0$	0.51 ± 0.01	195 ± 6
50	P_0	1	0.187	0.585	1.158	0.939	$0.5P_0$	0.38 ± 0.02	265 ± 13
			0.461	0.342	3.280	3.061	$0.5P_0$	0.51 ± 0.02	201 ± 7
		3	0.187	0.620	1.003	0.860	P_0	0.35 ± 0.03	289 ± 23
			0.461	0.420	2.361	2.142	$0.5P_0$	0.35 ± 0.01	287 ± 9
		5	0.187	0.648	0.870	0.728	P_0	0.29 ± 0.02	342 ± 18
			0.461	0.438	2.123	1.905	$0.5P_0$	0.31 ± 0.02	323 ± 16
		7	0.187	0.651	0.852	0.709	P_0	0.28 ± 0.02	351 ± 24
			0.461	0.443	2.088	1.869	$0.5P_0$	0.30 ± 0.01	329 ± 14
	$0.5P_0$	2	0.187	0.279	1.206	0.987	$0.5P_0$	0.40 ± 0.02	252 ± 11
			0.461	0.163	3.353	3.134	$0.5P_0$	0.51 ± 0.03	196 ± 10
		4	0.187	0.284	1.131	0.913	$0.5P_0$	0.37 ± 0.02	273 ± 18
			0.461	0.175	2.997	2.778	$0.5P_0$	0.45 ± 0.02	221 ± 9
		6	0.187	0.284	1.136	0.917	$0.5P_0$	0.37 ± 0.03	271 ± 19
			0.461	0.181	2.836	2.618	$0.5P_0$	0.43 ± 0.02	235 ± 9
		8	0.187	0.284	1.129	0.911	$0.5P_0$	0.37 ± 0.03	273 ± 25
			0.461	0.181	2.841	2.622	$0.5P_0$	0.43 ± 0.02	234 ± 10
80	P_0	1	0.187	0.565	1.247	0.943	$0.5P_0$	0.38 ± 0.03	264 ± 18
			0.461	0.353	3.096	2.792	$0.5P_0$	0.45 ± 0.02	220 ± 9
		3	0.187	0.624	0.948	0.716	P_0	0.29 ± 0.03	347 ± 31
			0.461	0.432	2.183	1.879	$0.5P_0$	0.31 ± 0.02	327 ± 16
		5	0.187	0.639	0.860	0.628	P_0	0.25 ± 0.02	396 ± 38
			0.461	0.454	1.953	1.649	$0.5P_0$	0.27 ± 0.02	373 ± 24
		7	0.187	0.632	0.886	0.654	P_0	0.26 ± 0.03	381 ± 38
			0.461	0.457	1.923	1.618	$0.5P_0$	0.26 ± 0.02	380 ± 22
	$0.5P_0$	2	0.187	0.251	1.472	1.167	$0.5P_0$	0.47 ± 0.04	213 ± 10
			0.461	0.159	3.477	3.172	$0.5P_0$	0.52 ± 0.02	194 ± 9
		4	0.187	0.265	1.248	0.943	$0.5P_0$	0.38 ± 0.03	264 ± 23
			0.461	0.175	2.918	2.614	$0.5P_0$	0.43 ± 0.02	235 ± 8
		6	0.187	0.262	1.305	1.001	$0.5P_0$	0.40 ± 0.04	249 ± 28
			0.461	0.179	2.824	2.520	$0.5P_0$	0.41 ± 0.02	244 ± 10
		8	0.187	0.260	1.319	1.015	$0.5P_0$	0.41 ± 0.04	245 ± 22
			0.461	0.179	2.834	2.530	$0.5P_0$	0.41 ± 0.02	243 ± 10

^a Each value is the average of 10 data points from 253–289 s. Errors are standard deviations.

Table S10. Values of k_{1-a} , k_{g-a} , and R_{g-a} for Successive Runs with Montmorillonite Sample

RH (%)	P_{in}	Run	S/S_c	$x_{out}(t)$ ^a	$10^2 k_{1-a} (\text{s}^{-1})$ ^a			k_{g-a} (cm s^{-1})	$R_{g-a} (\text{s m}^{-1})$	
					From eqn (21)	After blank correction	P_{in} for blank		value	average
20	P_0	1	0.187	0.614	1.047	0.967	P_0	0.39 ± 0.02	257 ± 13	256 ± 9
			0.461	0.405	2.516	2.408	$0.5P_0$	0.39 ± 0.02	255 ± 10	
		3	0.187	0.685	0.781	0.701	P_0	0.28 ± 0.02	355 ± 20	343 ± 16
			0.461	0.468	1.964	1.856	$0.5P_0$	0.30 ± 0.01	331 ± 7	
		5	0.187	0.712	0.675	0.595	P_0	0.24 ± 0.01	418 ± 25	
			0.461	0.501	1.689	1.581	$0.5P_0$	0.26 ± 0.01	389 ± 20	404 ± 22
		7	0.187	0.728	0.619	0.539	P_0	0.22 ± 0.02	462 ± 38	435 ± 33
	$0.5P_0$		0.461	0.513	1.614	1.505	$0.5P_0$	0.24 ± 0.01	409 ± 14	
		2	0.187	0.314	0.940	0.832	$0.5P_0$	0.33 ± 0.02	299 ± 15	279 ± 22
			0.461	0.200	2.486	2.377	$0.5P_0$	0.39 ± 0.01	259 ± 9	
		4	0.187	0.331	0.792	0.683	$0.5P_0$	0.27 ± 0.02	364 ± 29	328 ± 39
			0.461	0.213	2.212	2.103	$0.5P_0$	0.34 ± 0.01	292 ± 11	
		6	0.187	0.320	0.874	0.766	$0.5P_0$	0.31 ± 0.02	325 ± 17	
			0.461	0.224	1.981	1.872	$0.5P_0$	0.30 ± 0.01	328 ± 14	327 ± 11
50	P_0	8	0.187	0.338	0.726	0.617	$0.5P_0$	0.25 ± 0.02	403 ± 36	
			0.461	0.230	1.866	1.757	$0.5P_0$	0.29 ± 0.02	350 ± 19	377 ± 34
		1	0.187	0.622	1.005	0.863	P_0	0.35 ± 0.01	289 ± 12	
			0.461	0.379	2.764	2.545	$0.5P_0$	0.41 ± 0.02	242 ± 10	265 ± 25
		3	0.187	0.693	0.716	0.573	P_0	0.23 ± 0.02	434 ± 37	
			0.461	0.458	2.005	1.786	$0.5P_0$	0.29 ± 0.01	344 ± 11	389 ± 49
		5	0.187	0.717	0.620	0.477	P_0	0.19 ± 0.02	522 ± 47	
	$0.5P_0$		0.461	0.478	1.826	1.607	$0.5P_0$	0.26 ± 0.01	382 ± 12	452 ± 74
		7	0.187	0.718	0.598	0.455	P_0	0.18 ± 0.02	547 ± 54	
			0.461	0.490	1.686	1.468	$0.5P_0$	0.24 ± 0.01	419 ± 23	483 ± 71
		2	0.187	0.320	0.829	0.610	$0.5P_0$	0.25 ± 0.02	408 ± 39	
			0.461	0.179	2.937	2.718	$0.5P_0$	0.44 ± 0.02	226 ± 12	317 ± 93
		4	0.187	0.317	0.843	0.624	$0.5P_0$	0.25 ± 0.02	399 ± 40	
			0.461	0.197	2.475	2.257	$0.5P_0$	0.37 ± 0.01	272 ± 9	336 ± 39
80	P_0	6	0.187	0.319	0.822	0.603	$0.5P_0$	0.24 ± 0.02	413 ± 36	
			0.461	0.199	2.400	2.181	$0.5P_0$	0.35 ± 0.02	282 ± 16	347 ± 68
		8	0.187	no data						
			0.461	0.204	2.303	2.085	$0.5P_0$	0.34 ± 0.02	295 ± 17	
		1	0.187	0.580	1.190	0.886	$0.5P_0$	0.36 ± 0.02	281 ± 14	
			0.461	0.360	3.017	2.713	$0.5P_0$	0.44 ± 0.01	227 ± 6	254 ± 28
		3	0.187	0.633	0.938	0.706	P_0	0.28 ± 0.02	352 ± 21	
	$0.5P_0$		0.461	0.421	2.343	2.038	$0.5P_0$	0.33 ± 0.01	302 ± 12	344 ± 46
		5	0.187	0.642	0.887	0.656	P_0	0.26 ± 0.02	380 ± 25	
			0.461	0.449	2.047	1.743	$0.5P_0$	0.28 ± 0.01	353 ± 16	366 ± 20
		7	0.187	0.648	0.876	0.645	P_0	0.26 ± 0.02	386 ± 36	
			0.461	0.453	2.002	1.697	$0.5P_0$	0.28 ± 0.01	362 ± 18	374 ± 23
		2	0.187	0.266	1.332	1.028	$0.5P_0$	0.41 ± 0.03	242 ± 19	
			0.461	0.162	3.370	3.065	$0.5P_0$	0.50 ± 0.02	201 ± 8	221 ± 23
80	$0.5P_0$	4	0.187	0.276	1.209	0.905	$0.5P_0$	0.36 ± 0.03	275 ± 23	
			0.461	0.172	3.015	2.711	$0.5P_0$	0.44 ± 0.03	227 ± 13	255 ± 32
		6	0.187	0.278	1.192	0.888	$0.5P_0$	0.36 ± 0.03	280 ± 24	
			0.461	0.179	2.839	2.534	$0.5P_0$	0.41 ± 0.03	243 ± 18	261 ± 24
		8	0.187	0.275	1.186	0.882	$0.5P_0$	0.35 ± 0.03	282 ± 31	
			0.461	0.177	2.894	2.590	$0.5P_0$	0.42 ± 0.02	237 ± 13	260 ± 28

^a Each value is the average of 10 data points from 253–289 s. Errors are standard deviations.

Table S11. Values of k_{1-a} , k_{g-a} , and R_{g-a} for Successive Runs with Kaolinite Sample

RH (%)	P_{in}	Run	S/S_c	$x_{out}(t)$ ^a	$10^2 k_{1-a} (\text{s}^{-1})$ ^a		k_{g-a} (cm s^{-1})	$R_{g-a} (\text{s m}^{-1})$	
					From eqn (21)	After blank correction		value	average
20	P_0	1	0.187	0.480	1.833	1.724	$0.5P_0$	0.69 ± 0.03	144 ± 7
			0.461	0.348	3.303	3.194	$0.5P_0$	0.52 ± 0.01	192 ± 3
		3	0.187	0.556	1.352	1.243	$0.5P_0$	0.50 ± 0.02	200 ± 8
			0.461	0.387	2.793	2.685	$0.5P_0$	0.44 ± 0.01	229 ± 5
		5	0.187	0.541	1.438	1.330	$0.5P_0$	0.53 ± 0.02	187 ± 6
			0.461	0.398	2.644	2.536	$0.5P_0$	0.41 ± 0.01	242 ± 6
		7	0.187	0.542	1.394	1.285	$0.5P_0$	0.52 ± 0.01	194 ± 5
			0.461	0.400	2.598	2.490	$0.5P_0$	0.40 ± 0.01	247 ± 7
		2	0.187	0.233	1.820	1.712	$0.5P_0$	0.69 ± 0.05	145 ± 10
			0.461	0.168	3.333	3.224	$0.5P_0$	0.52 ± 0.01	191 ± 4
50	$0.5P_0$	4	0.187	0.235	1.783	1.674	$0.5P_0$	0.67 ± 0.03	149 ± 8
			0.461	0.179	3.026	2.917	$0.5P_0$	0.47 ± 0.02	211 ± 9
		6	0.187	0.231	1.812	1.703	$0.5P_0$	0.68 ± 0.04	146 ± 8
			0.461	0.178	3.017	2.909	$0.5P_0$	0.47 ± 0.02	211 ± 8
		8	0.187	0.228	1.867	1.758	$0.5P_0$	0.71 ± 0.03	142 ± 7
			0.461	no data					
		1	0.187	0.579	1.223	1.004	$0.5P_0$	0.40 ± 0.03	248 ± 18
			0.461	0.363	3.054	2.835	$0.5P_0$	0.46 ± 0.01	217 ± 5
		3	0.187	0.655	0.886	0.743	P_0	0.30 ± 0.01	335 ± 14
			0.461	0.426	2.361	2.143	$0.5P_0$	0.35 ± 0.01	287 ± 8
80	P_0	5	0.187	0.676	0.798	0.655	P_0	0.26 ± 0.01	380 ± 21
			0.461	0.472	1.902	1.684	$0.5P_0$	0.27 ± 0.01	365 ± 15
		7	0.187	0.699	0.689	0.546	P_0	0.22 ± 0.01	456 ± 27
			0.461	0.498	1.705	1.486	$0.5P_0$	0.24 ± 0.01	414 ± 10
		2	0.187	0.283	1.205	0.986	$0.5P_0$	0.40 ± 0.02	252 ± 10
			0.461	0.176	3.050	2.831	$0.5P_0$	0.46 ± 0.01	217 ± 6
		4	0.187	0.300	1.015	0.796	$0.5P_0$	0.32 ± 0.02	313 ± 20
			0.461	0.198	2.498	2.279	$0.5P_0$	0.37 ± 0.01	270 ± 10
		6	0.187	0.308	0.935	0.717	$0.5P_0$	0.29 ± 0.02	347 ± 27
			0.461	0.206	2.295	2.076	$0.5P_0$	0.34 ± 0.02	296 ± 16
50	$0.5P_0$	8	0.187	0.311	0.881	0.662	$0.5P_0$	0.27 ± 0.02	376 ± 29
			0.461	0.213	2.155	1.936	$0.5P_0$	0.31 ± 0.01	318 ± 15
		1	0.187	0.507	1.638	1.333	$0.5P_0$	0.54 ± 0.02	187 ± 8
			0.461	0.342	3.334	3.030	$0.5P_0$	0.49 ± 0.01	203 ± 5
		3	0.187	0.566	1.243	0.939	$0.5P_0$	0.38 ± 0.02	265 ± 12
			0.461	0.423	2.331	2.027	$0.5P_0$	0.33 ± 0.01	303 ± 11
		5	0.187	0.597	1.075	0.843	P_0	0.34 ± 0.02	295 ± 20
			0.461	0.460	1.980	1.675	$0.5P_0$	0.27 ± 0.01	367 ± 15
		7	0.187	0.602	1.035	0.804	P_0	0.32 ± 0.02	310 ± 19
			0.461	0.475	1.820	1.515	$0.5P_0$	0.25 ± 0.01	406 ± 22
80	P_0	2	0.187	0.231	1.785	1.480	$0.5P_0$	0.59 ± 0.03	168 ± 10
			0.461	0.161	3.428	3.123	$0.5P_0$	0.51 ± 0.02	197 ± 9
		4	0.187	0.242	1.608	1.304	$0.5P_0$	0.52 ± 0.04	191 ± 15
			0.461	0.181	2.819	2.515	$0.5P_0$	0.41 ± 0.02	244 ± 13
		6	0.187	0.242	1.586	1.282	$0.5P_0$	0.51 ± 0.04	194 ± 15
			0.461	0.186	2.643	2.338	$0.5P_0$	0.38 ± 0.02	263 ± 13
		8	0.187	0.247	1.526	1.222	$0.5P_0$	0.49 ± 0.03	204 ± 13
			0.461	0.189	2.554	2.250	$0.5P_0$	0.37 ± 0.02	273 ± 14

^a Each value is the average of 10 data points from 253–289 s. Errors are standard deviations.

Table S12. Values of k_{1-a} , k_{g-a} , and R_{g-a} for Successive Runs with Halloysite Sample

RH (%)	P_{in}	Run	S/S_c	$x_{out}(t)$ ^a	$10^2 k_{1-a} (\text{s}^{-1})$ ^a		k_{g-a} (cm s^{-1})	$R_{g-a} (\text{s m}^{-1})$	
					From eqn (21)	After blank correction		value	average
20	P_0	1	0.187	0.566	1.285	1.176	$0.5P_0$	0.47 ± 0.03	212 ± 11
			0.461	0.373	2.933	2.824	$0.5P_0$	0.46 ± 0.01	218 ± 6
		3	0.187	0.614	1.049	0.968	P_0	0.39 ± 0.02	257 ± 10
			0.461	0.440	2.188	2.079	$0.5P_0$	0.34 ± 0.01	296 ± 8
		5	0.187	0.613	1.053	0.972	P_0	0.39 ± 0.01	256 ± 9
			0.461	0.447	2.113	2.004	$0.5P_0$	0.33 ± 0.01	307 ± 12
		7	0.187	0.609	1.043	0.962	P_0	0.39 ± 0.02	259 ± 12
			0.461	0.442	2.149	2.040	$0.5P_0$	0.33 ± 0.01	301 ± 12
		2	0.187	0.274	1.273	1.164	$0.5P_0$	0.47 ± 0.03	214 ± 15
			0.461	0.185	2.825	2.717	$0.5P_0$	0.44 ± 0.01	226 ± 6
50	$0.5P_0$	4	0.187	0.278	1.222	1.114	$0.5P_0$	0.45 ± 0.04	224 ± 18
			0.461	0.196	2.534	2.425	$0.5P_0$	0.39 ± 0.01	253 ± 9
		6	0.187	0.279	1.240	1.131	$0.5P_0$	0.45 ± 0.02	220 ± 11
			0.461	0.195	2.542	2.433	$0.5P_0$	0.40 ± 0.02	253 ± 12
		8	0.187	0.273	1.318	1.209	$0.5P_0$	0.49 ± 0.03	206 ± 14
			0.461	0.193	2.616	2.507	$0.5P_0$	0.41 ± 0.01	245 ± 9
		1	0.187	0.579	1.177	0.959	$0.5P_0$	0.39 ± 0.02	260 ± 14
			0.461	0.414	2.373	2.154	$0.5P_0$	0.35 ± 0.01	285 ± 8
		3	0.187	0.677	0.723	0.581	P_0	0.23 ± 0.02	429 ± 32
			0.461	0.507	1.611	1.392	$0.5P_0$	0.23 ± 0.01	442 ± 22
80	P_0	5	0.187	0.672	0.737	0.594	P_0	0.24 ± 0.02	419 ± 28
			0.461	0.542	1.349	1.130	$0.5P_0$	0.18 ± 0.01	544 ± 26
		7	0.187	0.678	0.717	0.574	P_0	0.23 ± 0.02	434 ± 41
			0.461	0.547	1.303	1.085	$0.5P_0$	0.18 ± 0.01	567 ± 29
		2	0.187	0.274	1.238	1.020	$0.5P_0$	0.41 ± 0.03	244 ± 17
			0.461	0.196	2.462	2.243	$0.5P_0$	0.36 ± 0.02	274 ± 13
		4	0.187	0.285	1.092	0.874	$0.5P_0$	0.35 ± 0.03	285 ± 22
			0.461	0.218	2.003	1.785	$0.5P_0$	0.29 ± 0.01	344 ± 15
		6	0.187	0.284	1.094	0.875	$0.5P_0$	0.35 ± 0.02	284 ± 17
			0.461	0.223	1.917	1.699	$0.5P_0$	0.28 ± 0.02	362 ± 24
50	$0.5P_0$	8	0.187	0.286	1.061	0.842	$0.5P_0$	0.34 ± 0.04	296 ± 36
			0.461	0.222	1.917	1.699	$0.5P_0$	0.27 ± 0.02	362 ± 24
		1	0.187	0.529	1.412	1.108	$0.5P_0$	0.45 ± 0.03	225 ± 14
			0.461	0.387	2.682	2.378	$0.5P_0$	0.39 ± 0.02	259 ± 13
		3	0.187	0.590	1.080	0.776	$0.5P_0$	0.31 ± 0.03	321 ± 27
			0.461	0.474	1.814	1.509	$0.5P_0$	0.25 ± 0.01	407 ± 20
		5	0.187	0.607	1.003	0.771	P_0	0.31 ± 0.02	323 ± 23
			0.461	0.501	1.610	1.306	$0.5P_0$	0.21 ± 0.01	471 ± 28
		7	0.187	0.598	1.041	0.810	P_0	0.33 ± 0.03	308 ± 27
			0.461	0.507	1.544	1.239	$0.5P_0$	0.20 ± 0.01	496 ± 35
80	$0.5P_0$	2	0.187	0.229	1.788	1.484	$0.5P_0$	0.60 ± 0.05	168 ± 13
			0.461	0.172	3.027	2.722	$0.5P_0$	0.44 ± 0.02	226 ± 9
		4	0.187	0.235	1.684	1.380	$0.5P_0$	0.55 ± 0.03	180 ± 11
			0.461	0.184	2.684	2.379	$0.5P_0$	0.39 ± 0.02	258 ± 15
		6	0.187	0.236	1.668	1.364	$0.5P_0$	0.55 ± 0.03	183 ± 10
			0.461	0.193	2.465	2.161	$0.5P_0$	0.35 ± 0.02	284 ± 15
		8	0.187	0.234	1.673	1.368	$0.5P_0$	0.55 ± 0.05	182 ± 15
			0.461	0.194	2.454	2.150	$0.5P_0$	0.35 ± 0.02	286 ± 17
									234 ± 53

^a Each value is the average of 10 data points from 253–289 s. Errors are standard deviations.

Table S13. Values of k_{1-a} , k_{g-a} , and R_{g-a} for Successive Runs with AgroMAT AG-1 Sample

RH (%)	P_{in}	Run	S/S_c	$x_{out}(t)$ ^a	$10^2 k_{1-a} (\text{s}^{-1})$ ^a		k_{g-a} (cm s^{-1})	$R_{g-a} (\text{s m}^{-1})$	
					From eqn (21)	After blank correction		value	average
20	P_0	1	0.187	0.554	1.383	1.274	$0.5P_0$	0.51 ± 0.02	195 ± 7
			0.461	0.370	2.999	2.890	$0.5P_0$	0.47 ± 0.01	213 ± 4
		3	0.187	0.583	1.218	1.109	$0.5P_0$	0.45 ± 0.02	224 ± 11
			0.461	0.400	2.612	2.503	$0.5P_0$	0.41 ± 0.01	246 ± 5
		5	0.187	0.588	1.188	1.079	$0.5P_0$	0.43 ± 0.02	231 ± 10
			0.461	0.403	2.586	2.477	$0.5P_0$	0.40 ± 0.01	248 ± 7
		7	0.187	0.585	1.203	1.094	$0.5P_0$	0.44 ± 0.01	227 ± 6
			0.461	0.417	2.434	2.325	$0.5P_0$	0.38 ± 0.01	264 ± 5
		2	0.187	0.270	1.392	1.283	$0.5P_0$	0.51 ± 0.02	194 ± 6
			0.461	0.176	3.099	2.990	$0.5P_0$	0.49 ± 0.01	206 ± 6
50	$0.5P_0$	4	0.187	0.267	1.409	1.300	$0.5P_0$	0.52 ± 0.01	192 ± 5
			0.461	0.178	3.063	2.955	$0.5P_0$	0.48 ± 0.02	208 ± 7
		6	0.187	0.269	1.372	1.263	$0.5P_0$	0.51 ± 0.03	197 ± 12
			0.461	0.179	3.020	2.911	$0.5P_0$	0.47 ± 0.01	211 ± 5
		8	0.187	0.265	1.428	1.319	$0.5P_0$	0.53 ± 0.02	189 ± 9
			0.461	0.181	2.959	2.850	$0.5P_0$	0.46 ± 0.01	216 ± 6
		1	0.187	0.504	1.650	1.431	$0.5P_0$	0.57 ± 0.02	174 ± 7
			0.461	0.377	2.842	2.624	$0.5P_0$	0.43 ± 0.01	234 ± 6
		3	0.187	0.546	1.384	1.165	P_0	0.47 ± 0.02	214 ± 10
			0.461	0.407	2.483	2.264	$0.5P_0$	0.37 ± 0.01	272 ± 9
80	P_0	5	0.187	0.553	1.345	1.127	P_0	0.45 ± 0.02	221 ± 9
			0.461	0.406	2.498	2.280	$0.5P_0$	0.37 ± 0.01	270 ± 7
		7	0.187	no data					
			0.461	0.403	2.533	2.315	$0.5P_0$	0.37 ± 0.01	266 ± 6
		2	0.187	0.238	1.730	1.512	$0.5P_0$	0.61 ± 0.04	165 ± 10
			0.461	0.173	3.125	2.906	$0.5P_0$	0.47 ± 0.02	212 ± 9
		4	0.187	0.236	1.793	1.574	$0.5P_0$	0.63 ± 0.03	158 ± 9
			0.461	0.174	3.077	2.859	$0.5P_0$	0.47 ± 0.02	215 ± 11
		6	0.187	0.237	1.741	1.522	$0.5P_0$	0.61 ± 0.03	164 ± 7
			0.461	0.174	3.093	2.875	$0.5P_0$	0.47 ± 0.02	214 ± 9
0.5P ₀	P_0	8	0.187	0.250	1.553	1.334	$0.5P_0$	0.54 ± 0.02	187 ± 7
			0.461	0.174	3.061	2.843	$0.5P_0$	0.46 ± 0.01	216 ± 6
		1	0.187	0.479	1.830	1.526	$0.5P_0$	0.61 ± 0.03	163 ± 7
			0.461	0.319	3.745	3.440	$0.5P_0$	0.56 ± 0.02	179 ± 5
		3	0.187	0.522	1.519	1.215	$0.5P_0$	0.49 ± 0.02	205 ± 9
			0.461	0.361	3.071	2.766	$0.5P_0$	0.45 ± 0.01	222 ± 6
		5	0.187	0.522	1.507	1.202	$0.5P_0$	0.48 ± 0.02	207 ± 10
			0.461	0.366	2.975	2.671	$0.5P_0$	0.43 ± 0.01	230 ± 6
		7	0.187	0.514	1.574	1.270	$0.5P_0$	0.51 ± 0.02	196 ± 7
			0.461	0.370	2.912	2.608	$0.5P_0$	0.42 ± 0.01	236 ± 7
0.5P ₀	P_0	2	0.187	0.212	2.140	1.835	$0.5P_0$	0.74 ± 0.02	136 ± 5
			0.461	0.148	3.922	3.618	$0.5P_0$	0.59 ± 0.02	170 ± 5
		4	0.187	0.219	2.008	1.704	$0.5P_0$	0.68 ± 0.03	146 ± 6
			0.461	0.154	3.701	3.396	$0.5P_0$	0.55 ± 0.02	181 ± 5
		6	0.187	0.217	2.065	1.760	$0.5P_0$	0.71 ± 0.03	141 ± 7
			0.461	0.152	3.768	3.463	$0.5P_0$	0.56 ± 0.03	178 ± 8
		8	0.187	0.214	2.080	1.775	$0.5P_0$	0.71 ± 0.03	140 ± 5
			0.461	0.153	3.761	3.457	$0.5P_0$	0.56 ± 0.02	178 ± 7
									159 ± 19

^a Each value is the average of 10 data points from 253–289 s. Errors are standard deviations.

S7.5. Derivation of eqn (32). The partial pressure of I₂ above the surface was assumed to be $P_{I_2-s}(t)$ in quasi-steady state conditions when the uptake of I₂ occurred in the forward direction. Because the application of eqn (S24) assumes Langmuir-type adsorption, $P_{I_2-s}(t)$ is approximated by eqn (S25).

$$\frac{dP_{I_2-s}(t)}{dt} = k_m(P_{I_2}(t) - P_{I_2-s}(t)) - k_a \left\{ (1 - \theta(t)) \times P_{I_2-s}(t) - \frac{\theta(t)}{K_{ads}} \right\} \approx 0 \quad (S24)$$

$$P_{I_2-s}(t) = \frac{k_m P_{I_2}(t) + \frac{k_a}{K_{ads}} \theta(t)}{k_m + k_a(1 - \theta(t))} \quad (S25)$$

where k_a is the rate of adsorption of I₂ on the clay surface. Thus, the forward rate, U_f , is thus given by

$$U_f = k_m(P_{I_2}(t) - P_{I_2-s}(t)) = \frac{1}{\frac{1}{k_m} + \frac{1}{k_a(1 - \theta(t))}} \times \left(P_{I_2}(t) - \frac{\theta(t)}{K_{ads}(1 - \theta(t))} \right) \quad (S26)$$

Letting U_b be the backward rate, U_b is given similarly by $-U_f$. When adsorption proceeds very rapidly, that is, $k_m \ll k_a(1 - \theta(t))$, eqn (S26) is approximated by

$$U_f = -U_b = k_m \times \left(P_{I_2}(t) - \frac{\theta(t)}{K_{ads}(1 - \theta(t))} \right) \quad (S27)$$

Representation of the partial pressure of I₂ by $x_{out}(t)$ instead of P_{I_2} in eqn (S27) gives

$$U = \frac{k_m \times \left(x_{out}(t) - \frac{\theta(t)}{K_{ads}(1 - \theta(t))} \right)}{x_{out}(t)} \times x_{out}(t) \quad (S28)$$

where U and K_{ads} are the forward rate and the adsorption equilibrium coefficients for $x_{out}(t)$, which is the ratio of the partial pressure of I₂ to P_0 (4.0×10^{-7} atm). Based on analogy with eqn (S24), we assumed a $k_m(t)$ determined with eqn (32). It should be noted that k_{ma} in eqn (32) is a parameter used to determine $k_m(t)$ and may be larger than the actual values of k_m or $k_m(t)$.

S7.6. Parameters obtained in the simulation

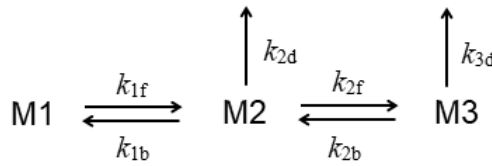
Table S14. Parameters used to reproduce both the time-series of $x_m(t)$ with small and large basins in runs 1–5 for each clay sample, RRS for each fitting result, and deposition rates and surface resistances calculated from them. Uncertainties of parameters are 90% at confidence level for the fitting procedure.

	RH (%)	Illite	Allophane	Mont-morillonite	Kaolinite	Halloysite	AgroMAT AG-1
k_{ma} (cm s ⁻¹)	20	7.42 ± 0.43	7.08 ± 0.56	2.24 ± 0.06	2.10 ± 0.24	1.18 ± 0.11	4.61 ± 0.79
	50	8.44 ± 0.80	2.47 ± 0.06	2.25 ± 0.03	1.58 ± 0.02	2.51 ± 0.16	1.22 ± 0.04
	80	1.81 ± 0.19	3.74 ± 0.20	3.48 ± 0.05	4.34 ± 0.36	5.51 ± 0.26	2.05 ± 0.05
K_{ads} (atm ⁻¹) [*]	20	1.34 ± 0.03	1.11 ± 0.04	0.75 ± 0.02	0.84 ± 0.06	0.54 ± 0.04	0.63 ± 0.02
	50	1.24 ± 0.02	1.07 ± 0.02	1.03 ± 0.01	0.81 ± 0.01	1.25 ± 0.03	0.74 ± 0.02
	80	1.17 ± 0.03	1.31 ± 0.03	1.27 ± 0.02	1.19 ± 0.02	1.59 ± 0.04	0.84 ± 0.02
$10^2 k_f$ (s ⁻¹)	20	1.38 ± 0.02	1.30 ± 0.03	1.16 ± 0.02	1.18 ± 0.05	1.21 ± 0.02	2.33 ± 0.03
	50	1.24 ± 0.02	0.77 ± 0.01	0.89 ± 0.01	1.05 ± 0.02	0.81 ± 0.03	1.47 ± 0.02
	80	0.77 ± 0.02	0.55 ± 0.02	0.69 ± 0.01	0.63 ± 0.02	0.59 ± 0.01	1.39 ± 0.03
K_{pads}	20	6.20 ± 0.12	5.06 ± 0.20	10.50 ± 0.34	4.09 ± 0.08	5.18 ± 0.21	12.70 ± 0.44
	50	5.44 ± 0.12	3.73 ± 0.10	5.08 ± 0.14	12.03 ± 0.56	1.95 ± 0.05	6.75 ± 0.11
	80	4.32 ± 0.15	1.78 ± 0.06	5.11 ± 0.15	4.05 ± 0.24	1.86 ± 0.04	6.78 ± 0.18
$10^3 k_{ls0}$ (s ⁻¹)	20	4.86 ± 0.08	5.31 ± 0.20	9.04 ± 0.14	8.53 ± 0.39	7.40 ± 0.19	6.09 ± 0.32
	50	4.79 ± 0.10	6.07 ± 0.11	8.12 ± 0.12	13.05 ± 0.19	7.91 ± 0.15	4.48 ± 0.16
	80	3.88 ± 0.09	5.59 ± 0.11	5.47 ± 0.09	7.65 ± 0.16	4.80 ± 0.07	5.84 ± 0.16
N_{ls0} [*]	20	3.23 ± 0.13	0.97 ± 0.08	1.11 ± 0.05	2.56 ± 0.28	0.75 ± 0.07	1.17 ± 0.15
	50	0.87 ± 0.06	1.04 ± 0.05	1.02 ± 0.03	1.93 ± 0.07	1.59 ± 0.04	0.58 ± 0.04
	80	0.68 ± 0.05	1.08 ± 0.04	1.01 ± 0.03	1.79 ± 0.10	1.05 ± 0.05	0.77 ± 0.07
$10^3 k_{loss-p}$ (s ⁻¹)	20	2.23 ± 0.02	2.04 ± 0.04	2.23 ± 0.04	2.61 ± 0.17	2.25 ± 0.05	2.33 ± 0.03
	50	2.02 ± 0.04	1.98 ± 0.04	2.16 ± 0.06	1.73 ± 0.06	2.18 ± 0.07	2.07 ± 0.03
	80	2.18 ± 0.04	1.94 ± 0.07	1.77 ± 0.04	1.71 ± 0.07	2.02 ± 0.06	2.34 ± 0.08
RSS	20	6497	18741	3770	31720	10989	4967
	50	5206	5524	3899	3181	6261	7079
	80	6044	6605	2940	6713	7844	9826
S/S_c		0.187	0.461	0.187	0.461	0.187	0.461
$10^3 q_\infty$ (nmol cm ⁻²)	20	0.87	0.70	1.32	0.88	0.73	1.33
	50	0.78	0.89	0.99	0.96	0.66	0.76
	80	1.18	1.07	1.09	0.97	0.84	0.82
k_{g0} (cm s ⁻¹)	20	0.79	0.64	0.94	0.63	0.54	0.53
	50	0.59	0.68	0.60	0.58	0.51	0.59
	80	0.65	0.59	0.64	0.57	0.58	0.57
k_g (cm s ⁻¹)	20	0.46	0.37	0.49	0.33	0.25	0.25
	50	0.32	0.37	0.23	0.22	0.19	0.22
	80	0.34	0.30	0.17	0.16	0.24	0.24
$R_{g-clay-0}$ (s m ⁻¹) ^{**}	20	141 ± 15	133 ± 26	186 ± 1	138 ± 29	178 ± 21	196 ± 17
	50	158 ± 11	168 ± 3	181 ± 14	156 ± 1	173 ± 28	188 ± 35
	80	161 ± 8	165 ± 9	173 ± 2	142 ± 23	167 ± 38	145 ± 20
R_{g-clay} (s m ⁻¹) ^{**}	20	241 ± 26	255 ± 51	402 ± 2	348 ± 74	401 ± 46	287 ± 25
	50	288 ± 20	440 ± 8	481 ± 36	447 ± 3	666 ± 107	305 ± 56
	80	308 ± 15	607 ± 34	414 ± 4	470 ± 77	515 ± 116	260 ± 36

* Unit is represented as a fraction of q_∞ .

** Uncertainties (±) are standard deviations of two values with $S/S_c = 0.187$ and 0.461.

S7.7. Derivation of eqn (37). The assumed scheme for the uptake process of I₂ on clay samples is illustrated in Scheme S1, where M1 is gaseous I₂, M2 is I₂ adsorbed on the surface in the first stage, and M3 is I₂ adsorbed in the interior in the second stage. Let n₁, n₂, and n₃ be concentrations of M1, M2, and M3, respectively, where the units of n₂ and n₃ are the same as the units of n₁. Values of n₁–n₃ are represented using variables in eqn (31)–(36) as shown in Table S15, because θ(t) and φ(t) are defined as a fraction of q_∞ and because q_∞ is represented by q_∞/B_{pm} if the unit of n₁ is used for q_∞. When n₁ is low (e.g., I₂ as in the atmosphere), each rate is expected to be proportional to each concentration of n₁, n₂, or n₃. Because k_m(t) assumes that exchanges between M1 and M2 are reversible (section S7.5), the parameters of k_{1f}, k_{1b}, k_{2f}, k_{2b}, k_{2d}, and k_{3d} in Scheme 1 are related to the parameters in eqn (31)–(36) (Table S15) for low concentrations of I₂.



Scheme S1. Scheme for process of uptake of I₂ onto clay samples.

Table S15. Comparison of variables and parameters between Scheme S1 and eqn (31)–(36)

Scheme S1	n ₁	n ₂	n ₃	k _{1f}	k _{1b}	k _{2f}	k _{2b}	k _{2d}	k _{3d}
eques 31–36	x _{out} (t)	$\frac{q_\infty}{B_{pm}}\theta(t)$	$\frac{q_\infty}{B_{pm}}\varphi(t)$	k _{ma}	$\frac{B_{pm}}{q_\infty}\frac{k_{ma}}{K_{ads}}$	k _f	$\frac{k_f}{K_{pads}}$	$k_{loss-s}(t)$	k_{loss-p}

Under steady state conditions, the uptake rate of M1, U_{M1}, and the first-order rate constant for the uptake, k_{1u}, are represented by

$$U_{M1} = k_{1u}n_1 = k_{2d}n_2 + k_{3d}n_3 \quad (S29)$$

Because M2–M3 are in steady states, the following equations were applied.

$$k_{1f}n_1 - (k_{1b} + k_{2f} + k_{2d}) \times n_2 + k_{2b}n_3 = 0 \quad (S30)$$

$$k_{2f}n_2 - (k_{2b} + k_{3f}) \times n_3 = 0 \quad (S31)$$

From eqn (S30) and (S31), n₂ and n₃ are given by n₁ as follows:

$$n_2 = \frac{k_{1f}(k_{2b} + k_{3d})}{k_{1b}k_{2b} + k_{1b}k_{3d} + k_{2f}k_{3d} + k_{2b}k_{2d} + k_{2d}k_{3d}} \times n_1 \quad (S32)$$

$$n_3 = \frac{k_{1f}k_{2f}}{k_{1b}k_{2b} + k_{1b}k_{3d} + k_{2f}k_{3d} + k_{2b}k_{2d} + k_{2d}k_{3d}} \times n_1 \quad (S33)$$

Substituting eqn (S32) and (S33) into eqn (S29) yields

$$U_{M1} = \left\{ \frac{\frac{k_{2d}}{\frac{1}{k_1} + \frac{k_{2d}}{k_{1f}(1 + \frac{k_{3d}}{k_{2b}})} + \frac{k_{2d}}{k_{1f}}}}{\frac{1}{k_1} + \frac{k_{2d}}{k_{1f}(1 + \frac{k_{3d}}{k_{2b}})} + \frac{k_{2d}}{k_{1f}}} + \frac{1}{\frac{1}{k_1} + \frac{1}{k_2} + \frac{1}{k_3} + k_{2d}\left(\frac{1}{k_2} + \frac{1}{k_3}\right)} \right\} \times n_1 \quad (S34)$$

where $K_1 = k_{1f}/k_{1b}$ and $K_2 = k_{2f}/k_{2b}$. From Table S15, eqn (S34) yields

$$U_{M1} = \left\{ \frac{\frac{q_\infty}{B_{pm}} k_{loss-s}(t)}{\frac{1}{K_{ads}} + \frac{1}{\frac{k_{ma}}{K_{pads} k_{loss-p}} + \frac{k_{ma}}{k_{2f}}} + \frac{\frac{q_\infty}{B_{pm}}}{\frac{1}{B_{pm}} \frac{1}{k_{ma}} + \frac{1}{K_{ads} k_f} + \frac{1}{K_{ads} K_{pads} k_{loss-p}} + \frac{k_{loss-s}(t)}{k_{ma} k_f} \left(\frac{k_f}{K_{pads} k_{loss-p}} + 1 \right)}} \right\} \times n_1 \quad (S35)$$

Comparing eqn (S35) with eqn (S29) gives eqn (37).

S7.8. Simulation of consecutive runs 1–5 for the same clay sample.

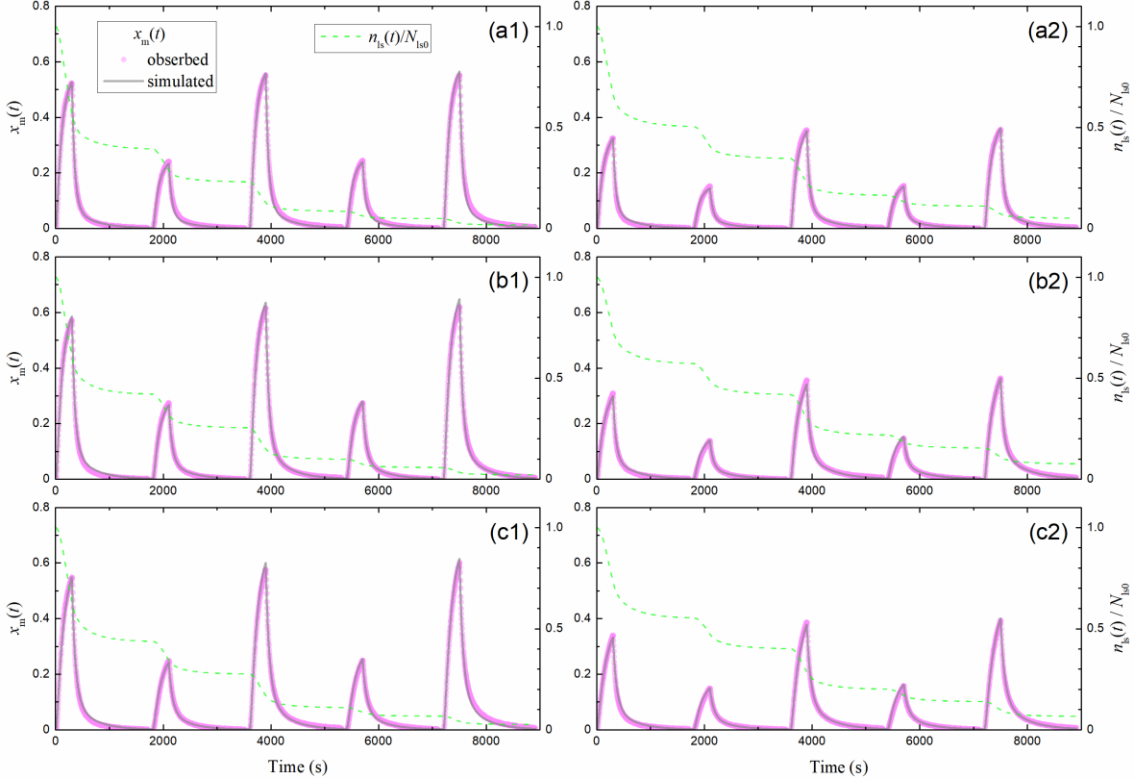


Figure S12. Time series of $x_m(t)$ in I₂-air(s) observed (pink circles) and simulated (grey curves) in runs 1–5 with each illite sample at (a) 20% RH, (b) 50% RH, and (c) 80% RH in small basins (S/S_c , 0.187; panels a1, b1, and c1) and large basins (S/S_c , 0.461; panels a2, b2, and c2). Dashed curves show time series of residence ratios of active sites for I₂ loss, $n_{ls}(t)/N_{ls0}$. Temporal duration of each run was about 1700 s and there were several minutes between runs; however, each panel plots all data of runs 1–5 in consecutive at 1800-s intervals for convenience.

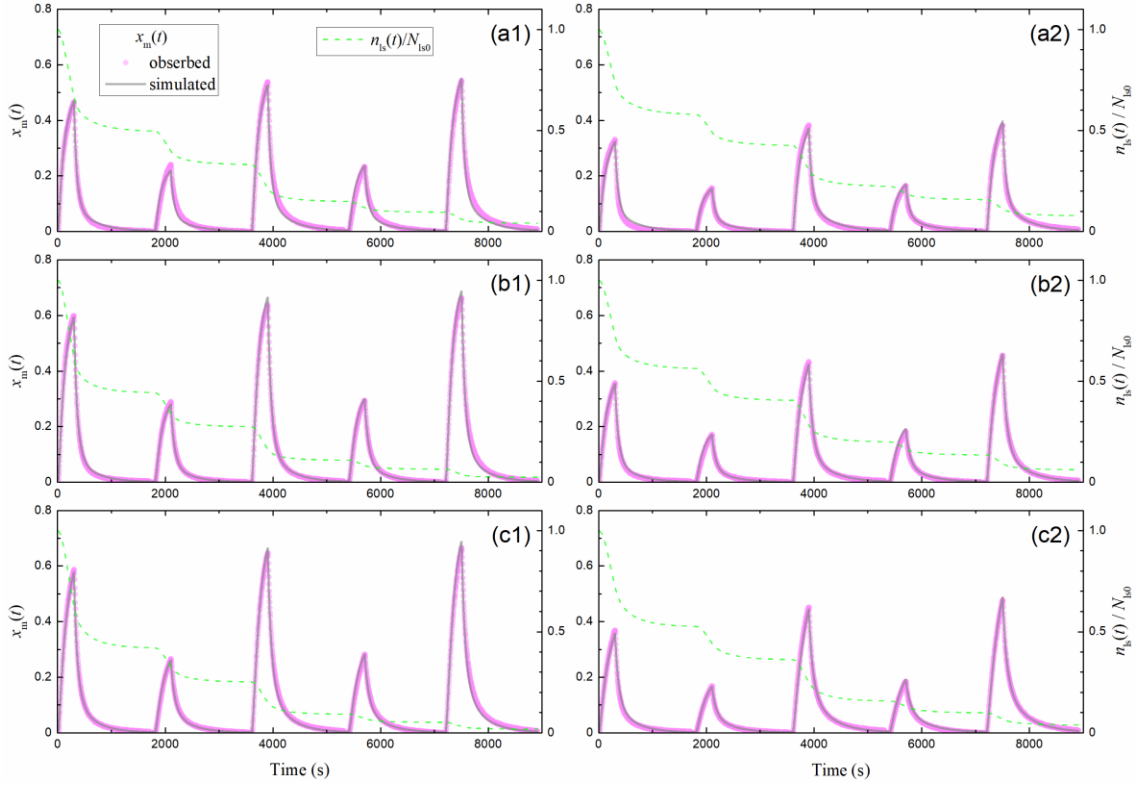


Figure S13. Same as Figure S12, but for runs 1–5 for allophane samples.

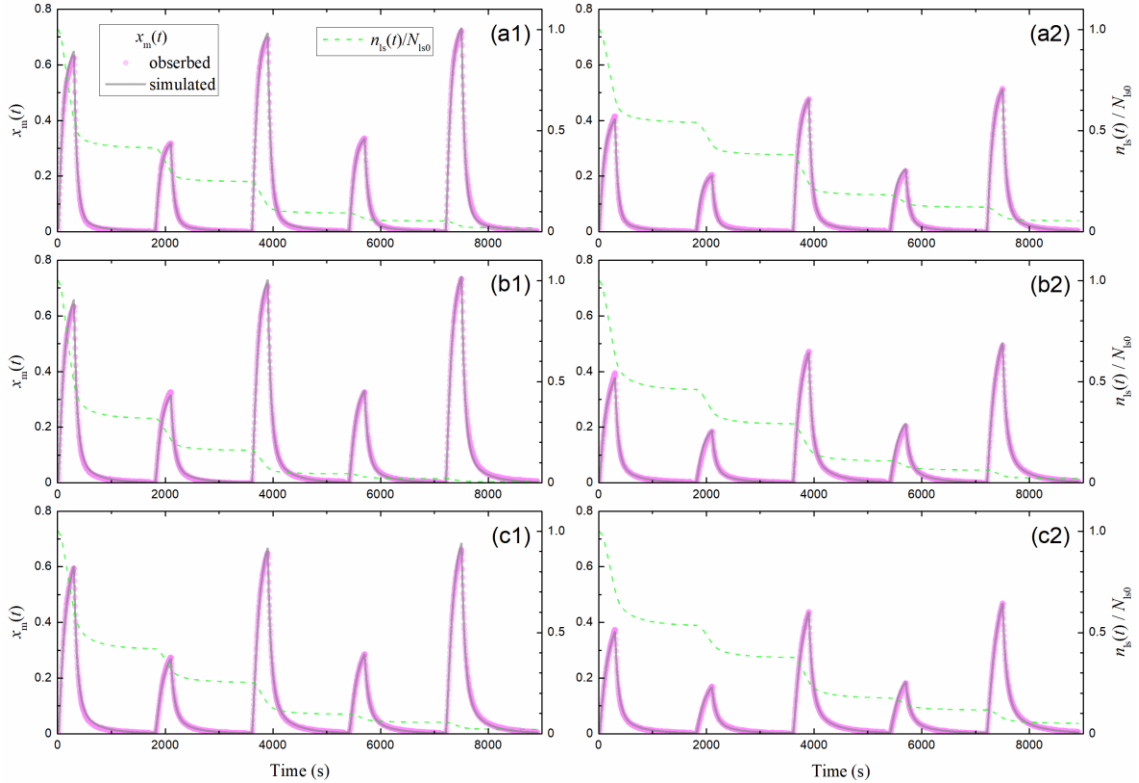


Figure S14. Same as Figure S12, but for runs 1–5 for montmorillonite samples.

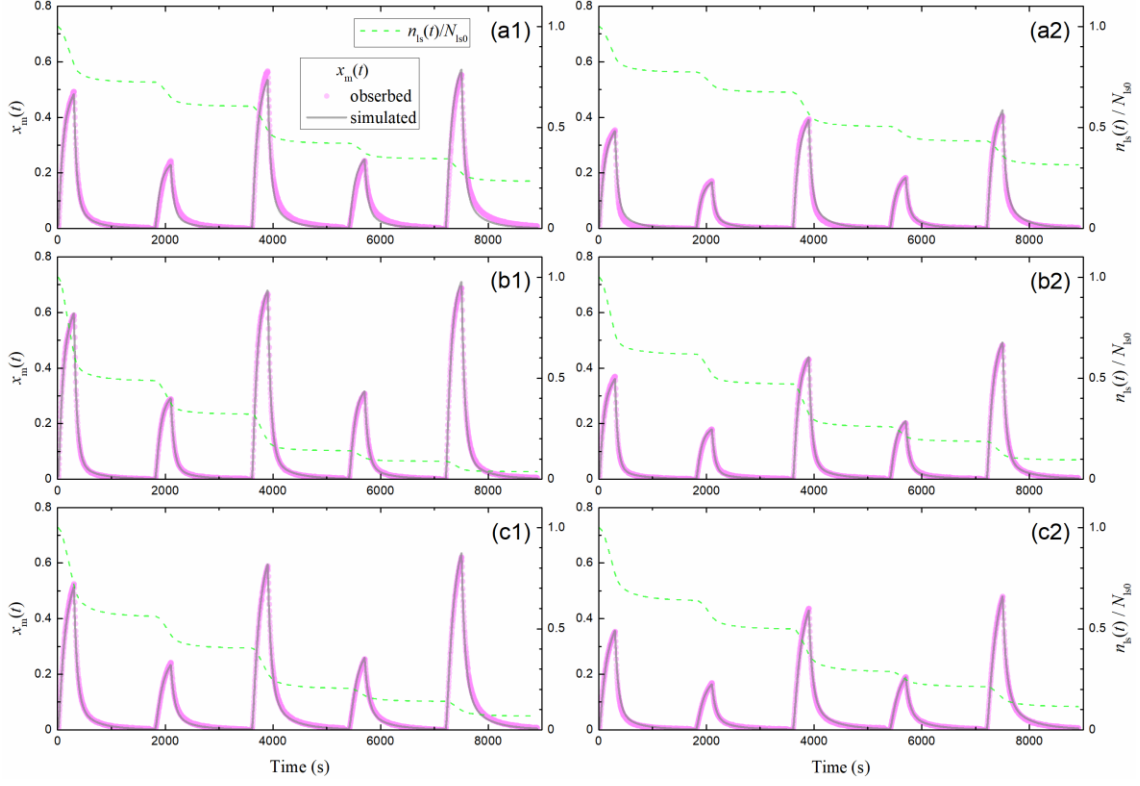


Figure S15. Same as Figure S12, but for runs 1–5 for kaolinite samples.

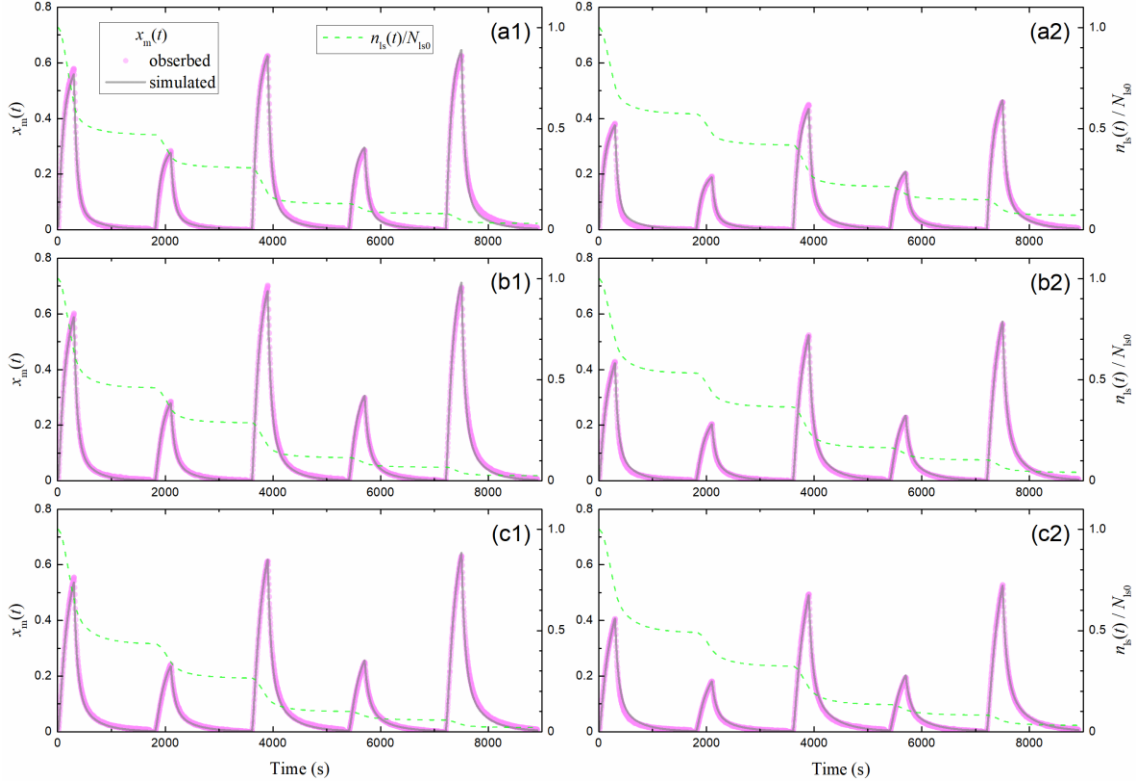


Figure S16. Same as Figure S12, but for runs 1–5 for halloysite samples.

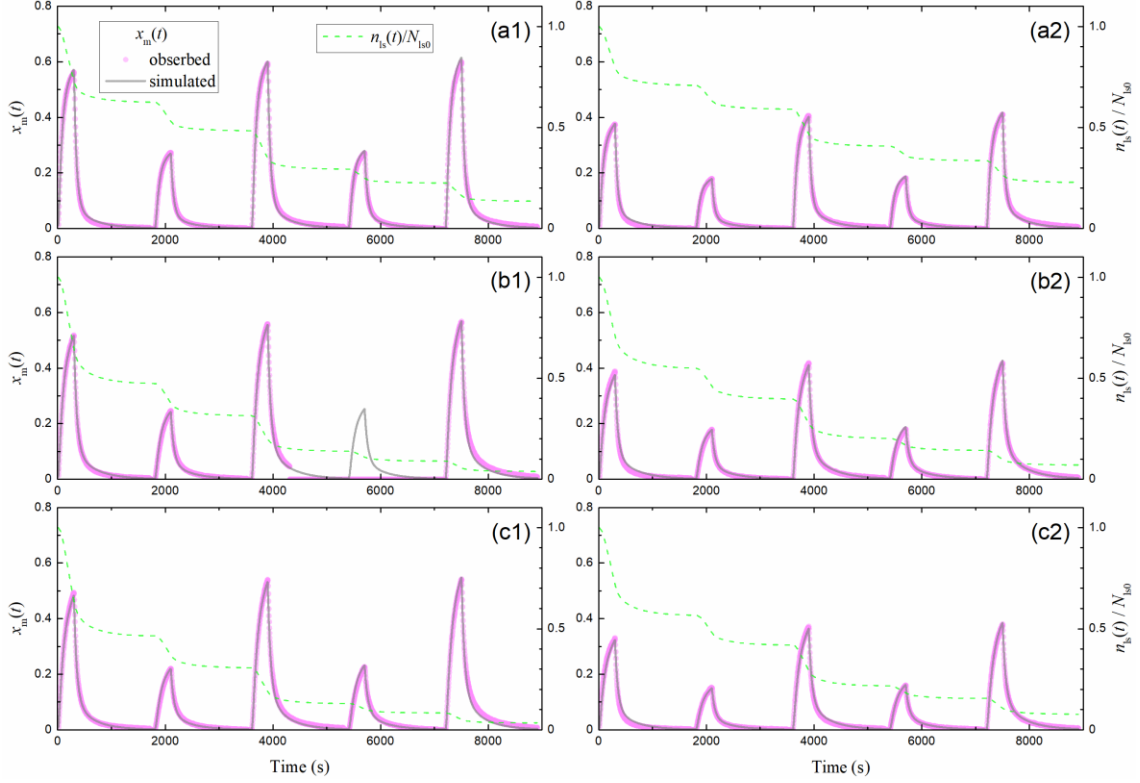


Figure S17. Same as Figure S12, but for runs 1–5 for AgroMAT AG-1 samples. The observed $x_m(t)$ data at 4313–7197 s with the small basin at 50% RH (panel b1) are missing because the baseline was changed at 713 s in run 3, and the data at 713–1709 s for run 3 and all data in run 4 are missing.

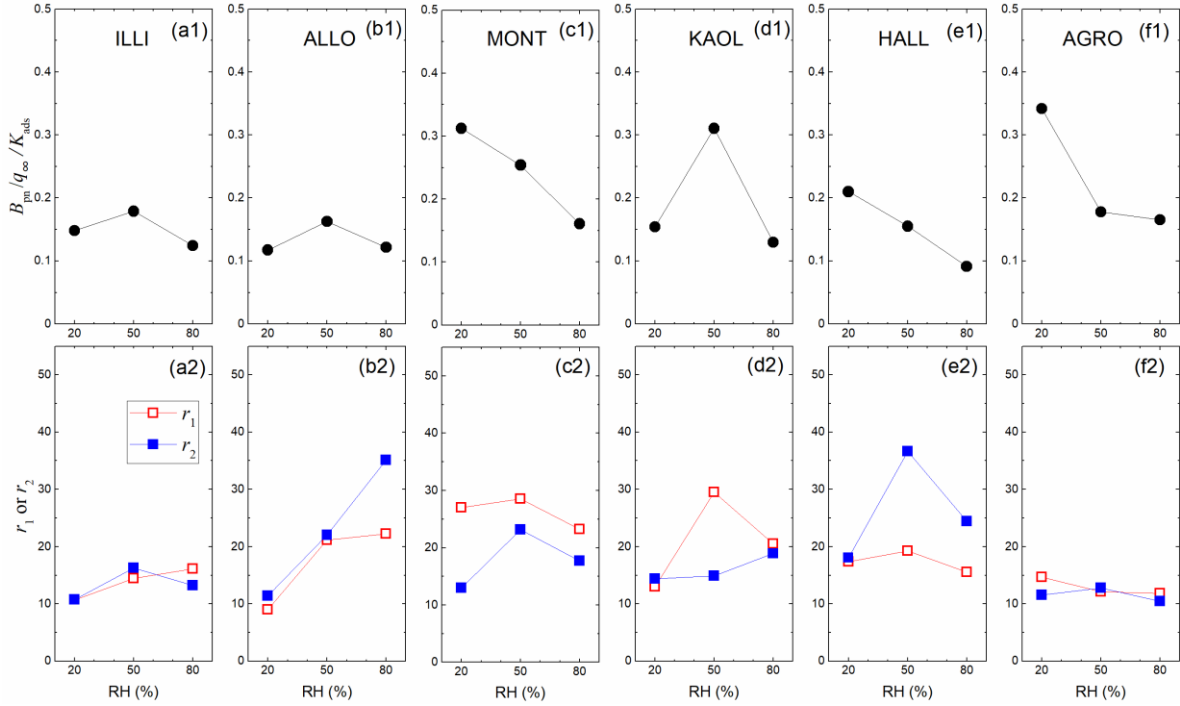


Figure S18. $B_{pn}/q_\infty/K_{ads}$ (panels 1), r_1 , and r_2 (panels 2) versus RH for I_2 -air(s) mixtures flowing over small basins of (a) illite, (b) allophane, (c) montmorillonite, (d) kaolinite, (e) halloysite, and (f) AgroMAT AG-1 samples. $B_{pn}/q_\infty/K_{ads}$, r_1 , and r_2 are calculated from the parameters obtained in the simulation (Table S14).

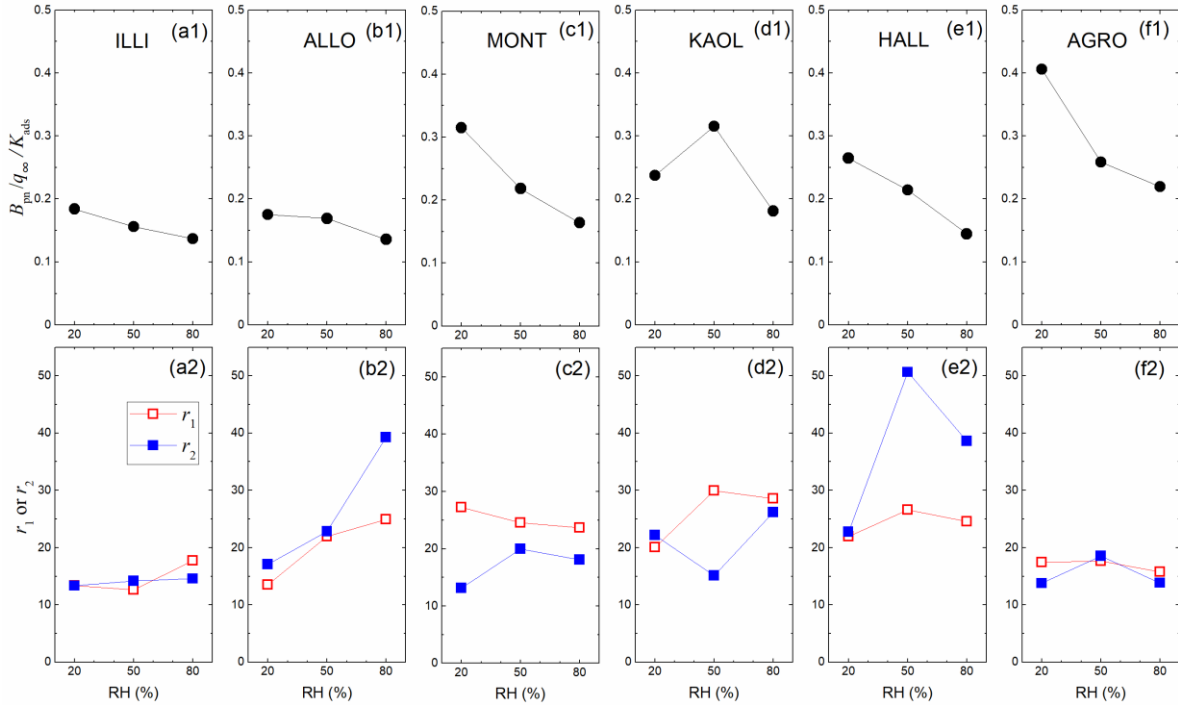


Figure S19. Same as Figure S18, but for I_2 -air(s) mixtures flowing over large basins.

S8. SUPPORTING INFORMATION FOR SECTION 3.4

S8.1. Parameters Used to Calculate Non-stomatal Resistance above each LUC.

Table S16. Reference Values of Parameters for Calculating Non-stomatal Resistance above LUCs⁸

	LUC		
	short grass and forbs	evergreen broadleaf trees	deciduous broadleaf trees
R_{ac0} (s m ⁻¹)	20	250	112
LAI	1	6	0.5
R_{cutd0} for SO ₂ (s m ⁻¹)	1000	2500	2500
R_g for SO ₂ (s m ⁻¹)	200	100	200
roughness length, z_0 (m)	0.04	2.0	0.4–1.0

In Table S16, R_{ac0} for deciduous broadleaf trees is calculated by

$$R_{ac0}(t) = R_{ac0}(\text{min}) + \frac{LAI(t) - LAI(\text{min})}{LAI(\text{max}) - LAI(\text{min})} \times [R_{ac0}(\text{max}) - R_{ac0}(\text{min})] \quad (\text{S36})$$

where $R_{ac0}(t)$ represents the R_{ac0} value at any day of the year and is set at a day in March; $R_{ac0}(\text{min})$ and $R_{ac0}(\text{max})$ are minimum and maximum R_{ac0} values for deciduous broadleaf trees and are 100 and 250 s m⁻¹, respectively; $LAI(t)$ is 0.5, the reference value of LAI in March; $LAI(\text{min})$ and $LAI(\text{max})$ are minimum and maximum LAI values and are 0.1 and 5, respectively, as seen in Figure 2 of Zhang et al.⁸

Values of u_* are related to the wind velocity (u_A , in m s⁻¹) at a certain altitude (z_A , in m) by

$$u_* = \frac{\kappa u_A}{\ln(z_A/z_0)} \quad (\text{S37})$$

where κ is von Karmen's constant, equal to 0.4, and z_0 is roughness length. Table S17 lists the u_* values calculated from the u_A values at 10 m height for each LUC by eqn (S37).

Table S17. Values of u_* for Each LUC

u_A at 10 m (m s ⁻¹)	u_* (m s ⁻¹)		
	Short grass and forbs	Evergreen broadleaf trees	Deciduous broadleaf trees
2	0.14	0.50	0.25–0.35
4	0.29	0.99	0.50–0.69
6	0.43	1.49	0.75–1.04
8	0.58	1.99	0.99–1.39
10	0.72	2.49	1.24–1.74
12	0.87	2.98	1.49–2.08
14	1.01	3.48	1.74–2.43
16	1.16	3.98	1.99–2.78
18	1.30	4.47	2.24–3.13
20	1.45	4.97	2.49–3.47

References

1. I. Sanemasa, T. Kobayashi, Y. P. Cheng and T. Deguchi, Equilibrium solubilities of iodine vapor in water, *Bull. Chem. Soc. Jpn.*, 1984, **57**, 1352-1357.
2. T. L. Allen and R. M. Keefer, The formation of hypoidous acid and hydrated iodine cation by the hydrolysis of iodine, *J. Am. Chem. Soc.*, 1955, **77**, 2957-2960.
3. R. Sander, Compilation of Henry's law constants (version 4.0) for water as solvent, *Atmos. Chem. Phys.*, 2015, **15**, 4399-4981.
4. W. Eguchi, M. Adachi and M. Yoneda, Dependency of partition equilibrium of iodine between air and aqueous solution containing sodium hydroxide upon temperature and concentration, *J. Chem. Eng. Jpn.*, 1974, **6**, 389-396.
5. C. R. Reid, J. M. Prausnitz and B. E. Poling, *The properties of gases and liquids*, 5th edn., McGraw-Hill, New York, 1987.
6. A. Takami, T. Kondo, A. Kado and S. Koda, The uptake coefficient of I₂ on various aqueous surfaces, *J. Atmos. Chem.*, 2001, **39**, 139-153.
7. A. E. Burgess and J. C. Davidson, Kinetics of the rapid reaction between iodine and ascorbic acid in aqueous solution using UV–Visible absorbance and titration by an iodine clock, *J. Chem. Educ.*, 2014, **91**, 300-304.
8. L. Zhang, J. R. Brook and R. Vet, A revised parameterization for gaseous dry deposition in air-quality models, *Atmos. Chem. Phys.*, 2003, **3**, 2067-2082.